Histological Study

To examine the complications to the retina or choroid from the transretinal electrical stimulation, or from the insertion and placement of the array itself, a histological study was performed on tissues adjacent to the areas where the electrode was placed. After examination of the EEP with electrical stimulation, the array was removed from the eyes and the rabbits were killed with a 5-ml intravenous injection of pentobarbital (50 mg/ml). The eyes were enucleated, dissected, and embedded in paraffin after incubation in 4% paraformaldehyde. Three-micrometer-thick paraffin sections were stained with H&E. The sections were examined by light microscopy, and the images were digitized using a CCD camera (AxioCam, Carl Zeiss Japan, Tokyo, Japan) and processed with AxioVision 2.0 (Carl Zeiss Japan) software on a Windows computer.

Results

The Electrode Array Under the Retina and Choroid

With a surgical microscope, the electrode array could be clearly seen under the retinal and choroidal vessels in the posterior portion of the eye. There were no major complications, such as retinal detachment, around the top of the array at the posterior portion (Fig. 3C).

The EEP with Varied Transretinal Electrical Stimulation

The EEP from all five eyes could be recorded with transretinal electrical stimulation. An example of an EEP with two types of biphasic current from an eye is shown in Fig. 4. The waves on the right were obtained with the biphasic pulse consisting of one current (suprachoroid to vitreous) and a second opposing current (vitreous to suprachoroid). Those on the left were obtained when the pulse consisted of opposite components. The smallest threshold from each of the five eyes was 66.0 ± 32.1 μA and 94.0 ± 68.4 μA (average ± SD) for each current direction, respect ($n = 5$) There was no statistical difference between different polarities ($P > 0.05$). With the superficial dimension, the averaged electrical density was 42.0 μC/cm^2 and 59.8 μC/cm^2, respectively. The implicit times of the first positive waves of the EEP with the two types of biphasic current were 9.0 ± 1.0 and 8.7 ± 0.9 ms, respectively (Fig. 4), and there was no statistical difference between polarities.

The Comparison Between Bright-flash VEP and the EEP

Bright-flash VEP waves were obtained from all five eyes, and the implicit time of the first positive wave was 21.7 ± 0.6 ms (average ± SD; Fig. 5, top). They were statistically longer than those of the EEP (Fig. 5, bottom, $P < 0.001$). The waveform of the EEP resembled the VEP waveform.

After cutting the optic nerve behind the eyes, the wave was not different from the baseline (data not shown).

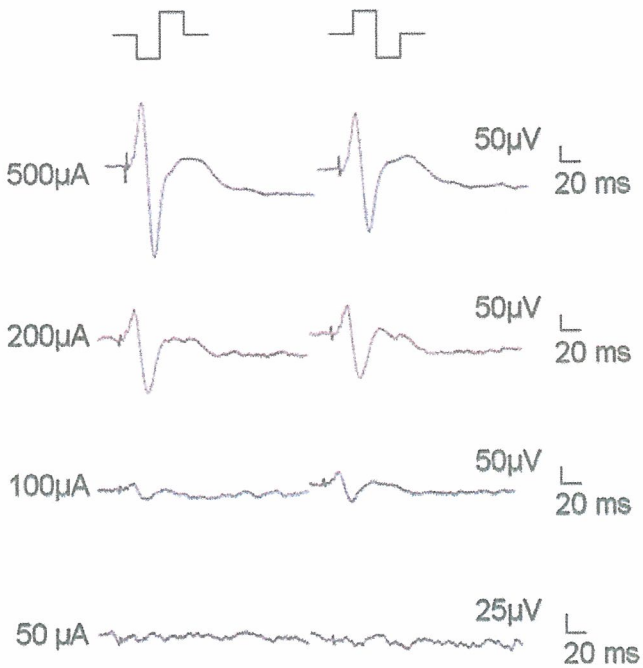

Figure 4. The electrical evoked potential (EEP) from a rabbit eye by transretinal electrical stimulation. *Left*: EEP waves obtained with a biphasic current consisting of suprachoroid to vitreous transretinal electrical stimulation and vitreous to suprachoroid stimulation. *Right*: EEP waves with currents with opposite polarization.

Histological Study

Histological examination of the sections around the suprachoroidal space into which the flat electrode array had been inserted demonstrated no severe complications such as retinal detachment after the insertion of the array and after a series of electrical stimulations (Fig. 6A).

Discussion

In this study, we developed a flat electrode array and were able to safely insert the array into the suprachoroidal space of albino rabbits. We performed the insertion into this space in the posterior portion of the eyes through a scleral incision at the limbus. We also showed that transretinal electrical stimulation from the suprachoroidal space could elicit an EEP.

Several methods can be used to stimulate the visual neurons for visual prosthesis: stimulation at the visual cortex, and stimulation of retinal neurons from a subretinal

Jpn J Ophthalmol
Vol 48: 256–261, 2004

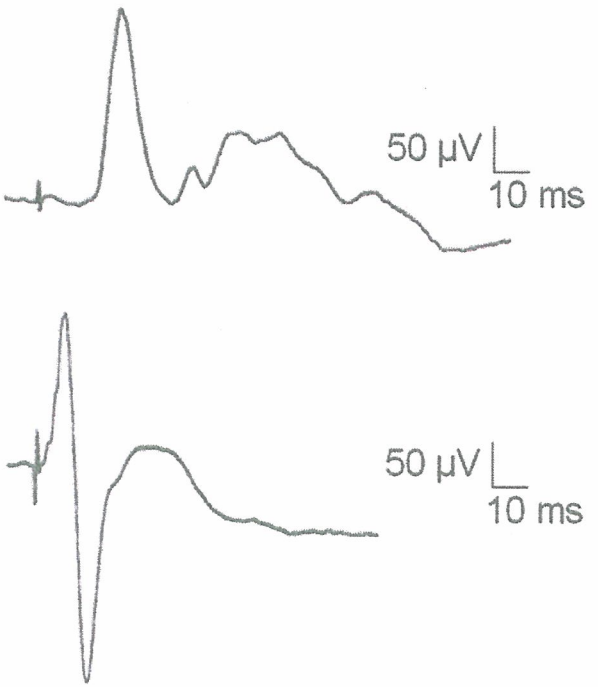

Figure 5. Comparison of waveforms between bright-flash visual evoked potential (VEP) and the electric evoked potential (EEP) from a rabbit eye. *Top*: A VEP wave consists of several positive waves. The implicit time of the first positive wave was 22.0 ms. *Bottom*: An EEP wave also consists of several positive waves. The implicit time of the first positive wave was 9.0 ms.

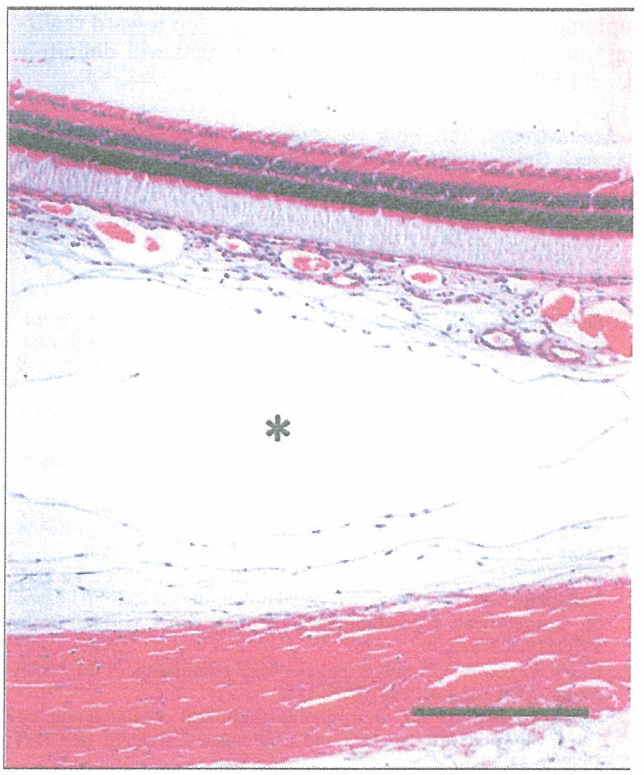

Figure 6. Results of the histological study of the suprachoroidal space where the flat electrode array was placed. The area around the space where the electrode array was placed (*) demonstrates no major complications such as retinal detachment or bleeding from the insertion of the array or after a series of electrical stimulations. Bar = 250 μm.

space or from the epiretinal side. On group also successfully developed a method for stimulation of the optic nerve in front of the chiasma.[20] All methods except stimulation of the retina require intracranial surgery, which has the risk of severe complications. Our method does not require intracranial surgery, and the insertion of the electrode into the suprachoroidal space is thought to be safer than the methods requiring intracranial surgery.

When the electrodes are placed at the epiretinal lesion or in the subretinal space, retinal detachment may occur. Because our method is not dependent upon the attachment of the array to the retina itself, it is comparatively safer.

Histological analysis in this study showed the separation of the choroidal tissues and sclera. This separation could lead to the breaking of the choroidal vessels and hemorrhage. Our short-term study showed no distinct hemorrhage around the top of the electrode array. A long-term study is required in the future to confirm this result.

The EEP waveforms by transretinal electrical stimulation resembled those of the bright-flash VEP. Implicit time of the EEP was 9.0 ± 1.0 or 8.7 ± 0.9 ms for each polarized biphasic pulse, and was statistically shorter compared with that of the flash VEP wave (21.7 ± 0.6 ms). This difference may be because of the longer time it takes for the flash of light to reach the photoreceptors and for the generated signal to travel along the nerves to the ganglion cells. The transretinal electrical current can stimulate the ganglion cells and nerve fibers directly.

It has been reported that the threshold of electrical density with an epiretinal implant is 1 to 12 $\mu C/cm^2$,[18] It has also been demonstrated that the threshold with a subretinal implant is 70 $\mu C/cm^2$,[9] According to these data, the threshold in our study is almost as low as that with a subretinal implant. With the subretinal implant, the photoreceptors or the bipolar cells are thought to be stimulated. With the epiretinal implant, the nerve fiber and ganglion cell layers may be stimulated. Although our device can stimulate each layer in the retina, including the nerve fiber and ganglion cell layers, with transretinal electrical stimulation, the choroidal tissues could cause resistance. This is a possible reason why the threshold in our study is much higher than that for an epiretinal implant. In contrast, because of the transretinal electrical stimulation, our device can be used with patients suffering from diseases involving severe damage to the photoreceptor layer, such as retinitis pigmentosa.

We demonstrated the possibility of using this flat electrode array for a visual prosthesis. To utilize this device in blind people, safety precautions for long-term electrode

placement in the eyes are required. We believe that this flat suprachoroidal electrode is a significant step toward realizing our goal of providing a prosthesis that will definitely benefit blind patients.

Acknowledgment. This work was supported by a Health Sciences Research Grant, Ministry of Health, Labor, and Welfare, Japan.

References

1. Dobelle WH, Mladejovsky MG. Phosphenes produced by electrical stimulation of human occipital cortex, and their application to the development of a prosthesis for the blind. J Physiol 1974;243:553–576.
2. Zrenner E. Will retinal implants restore vision? Science 2002;295:1022–1025.
3. Dobelle WH. Artificial vision for the blind by connecting a television camera to the visual cortex. ASAIO J 2000;46:3–9.
4. Normann RA, Warren DJ, Ammermuller J, Fernandez E, Guillory S. High-resolution spatio-temporal mapping of visual pathways using multi-electrode arrays. Vision Res 2001;41:1261–1275.
5. Schmidt EM, Bak MJ, Hambrecht FT, Kufta CV, O'Rourke DK, Vallabhanath P. Feasibility of a visual prosthesis for the blind based on intracortical microstimulation of the visual cortex. Brain 1996;119:507–522.
6. Chow AY, Chow VY. Subretinal electrical stimulation of the rabbit retina. Neurosci Lett 1997;225:13–16.
7. Peachey NS, Chow AY. Subretinal implantation of semiconductor-based photodiodes: progress and challenges. J Rehabil Res Dev 1999;36:371–376.
8. Peyman G, Chow AY, Liang C, Chow VY, Perlman JI, Peachey NS. Subretinal semiconductor microphotodiode array. Ophthalmic Surg Lasers 1998;29:234–241.
9. Schwahn HN, Gekeler F, Kohler K, et al. Studies on the feasibility of a subretinal visual prosthesis: data from Yucatan micropig and rabbit. Graefes Arch Clin Exp Ophthalmol 2001;239:961–967.
10. Zrenner E, Miliczek KD, Gabel VP, et al. The development of subretinal microphotodiodes for replacement of degenerated photoreceptors. Ophthalmic Res 1997;29:269–280.
11. Eckmiller R. Learning retina implants with epiretinal contacts. Ophthalmic Res 1997;29:281–289.
12. Walter P, Szurman P, Vobig M, et al. Successful long-term implantation of electrically inactive epiretinal microelectrode arrays in rabbits. Retina 1999;19:546–552.
13. Humayun MS, de Juan E Jr, Dagnelie G, Greenberg RJ, Propst RH, Phillips DH. Visual perception elicited by electrical stimulation of retina in blind humans. Arch Ophthalmol 1996;114:40–46.
14. Humayun MS, de Juan E Jr, Weiland JD, et al. Pattern electrical stimulation of the human retina. Vision Res 1999;39:2569–2576.
15. Santos A, Humayun MS, de Juan E Jr, et al. Preservation of the inner retina in retinitis pigmentosa. A morphometric analysis. Arch Ophthalmol 1997;115:511–515.
16. Grumet AE, Wyatt JL Jr, Rizzo JF 3rd. Multi-electrode stimulation and recording in the isolated retina. J Neurosci Methods 2000;101:31–42.
17. Rizzo JF 3rd, Wyatt J, Humayun M, et al. Retinal prosthesis: an encouraging first decade with major challenges ahead. Ophthalmology 2001;108:13–14.
18. Walter P, Heimann K. Evoked cortical potentials after electrical stimulation of the inner retina in rabbits. Graefes Arch Clin Exp Ophthalmol 2000;238:315–318.
19. Yanagida K, Miyake Y. Electrically Evoked Response (EER) in the rabbit. Nippon Ganka Gakkai Zasshi (Acta Soc Ophthalmol Jpn) 1984;88:997–1006.
20. Veraart C, Raftopoulos C, Mortimer JT, et al. Visual sensations produced by optic nerve stimulation using an implanted self-sizing spiral cuff electrode. Brain Res 1998;813:181–186.

Graefe's Arch Clin Exp Ophthalmol
(2005) 243: 169–174

LABORATORY INVESTIGATION

DOI 10.1007/s00417-004-1060-2

Kazuaki Nakauchi
Takashi Fujikado
Hiroyuki Kanda
Takeshi Morimoto
Jun S. Choi
Yasushi Ikuno
Hirokazu Sakaguchi
Motohiro Kamei
Masahito Ohji
Tohru Yagi
Shigeru Nishimura
Hajime Sawai
Yutaka Fukuda
Yasuo Tano

Transretinal electrical stimulation by an intrascleral multichannel electrode array in rabbit eyes

Received: 5 January 2004
Revised: 11 June 2004
Accepted: 19 September 2004
Published online: 7 December 2004

H.K., T.Y., and S.N. are employees of NIDEK Co.

K. Nakauchi · T. Fujikado (✉) ·
H. Kanda · T. Morimoto
Department of Visual Science, Osaka University Graduate School of Medicine,
Room G4, 2-2 Yamadaoka, Suita-shi, Osaka, 565-0871, Japan
e-mail: fujikado@ophthal.med.osaka-u.ac.jp
Tel.: +81-6-68793941
Fax: +81-6-68793948

J. S. Choi · Y. Ikuno · H. Sakaguchi · M. Kamei · M. Ohji · Y. Tano
Department of Ophthalmology, Osaka University Graduate School of Medicine,
Suita,
Osaka, Japan

H. Sawai · Y. Fukuda
Department of Physiology, Osaka University Graduate School of Medicine,
Suita,
Osaka, Japan

H. Kanda · T. Yagi · S. Nishimura
NIDEK Co.,
Gamagori, Japan

Abstract *Background:* A new method of stimulating the retina electrically, called suprachoroidal transretinal stimulation (STS), was shown to be effective in eliciting electrically evoked cortical potentials (EEPs) in Royal College of Surgeons (RCS) rats. Before extending this technique to patients, it is important to determine its safety and feasibility in eliciting EEPs from medium-size animal (rabbits). The purpose of this study was to determine the safety and efficacy of the surgical procedures used to implant an multichannel electrode array into a scleral pocket, and to determine whether the implanted electrodes can stimulate the retina effectively. *Methods:* These acute experiments were conducted on six rabbits. An array of eight gold microelectrodes, embedded in polyimide, was implanted into a scleral pocket over the visual streak area. The size of the microarray was 2×4×0.180 mm. The reference electrode was implanted into the vitreous. The electrode array and reference electrodes were connected to a stimulator to deliver monophasic current pulses. Cortical responses were recorded with a stainless steel electrode implanted into each rabbit's skull over the visual cortex. After the experiment, the eyes and electrodes were examined histologically. *Results:* The surgical procedures for electrode implantation were accomplished without serious complications. EEPs were recorded after monophasic electrical pulse stimulation from each electrode. The mean threshold for EEPs was 55.0±10.0 μA with a 0.5-ms duration inward current pulse. The charge delivered at threshold was about 27.5 nC, and the charge density was about 56.0 $\mu C/cm^2$. Histopathological examination of the retinal tissue around the area of stimulation did not show damage at the light microscope level with the electrical parameters used. *Conclusions:* Our technique for STS with an intrascleral microelectrode array is safe in rabbit eyes, and EEPs were elicited by current densities that did not induce tissue damage. These results suggest that STS via intrascleral multichannel electrodes is a feasible method for stimulating the retina.

Introduction

Several research groups are currently developing electrode arrays that can be attached directly to the retina and used to stimulate the retina in an attempt to restore vision to patients with retinal degeneration [7, 11, 18]. In general, there are two types of retinal stimulating prosthesis: an epiretinal [5, 6, 10, 13, 16] and a subretinal [2, 3, 14, 17] prosthesis. Epiretinal stimulating prostheses are inserted into the vitreous cavity and attached to or placed against the inner retinal surface. The potential risk of this approach is the possible of a permanent attachment of the device to the retina. Epiretinal implantation can cause damage around the area of the retinal plug [10, 15] or may be unstable without the use of special methods to fix the electrodes [18]. Subretinal prostheses are placed between the pigment epithelial layer and the outer layer of the retina. The stability of this electrode is better but chronic implantation in this space might lead to a proliferation of glial tissue around the electrode array [17]. Although improvements in the surgical and electronic technologies may solve some of the problems of implanting retinal stimulating prostheses, the potential risk of significant damage to the eye after inserting an electrode intraocularly is significant.

To avoid the risks of damaging the retina by implanting a stimulating electrode array into the epi- or subretinal space, we have developed a new method of stimulating the retina called suprachoroidal transretinal stimulation (STS), with implantation of a stimulating electrode array in the suprachoroidal space. This method avoids direct contact of the electrodes with the retina. We have demonstrated that STS can elicit field responses at a defined areas of the superior colliculus which correspond retinotopically to the retinal region stimulated in both normal and blind Royal College of Surgeons (RCS) rats [9].

In the present study, we fabricated a multichannel electrode array and developed a surgical technique to insert the electrodes in a scleral pocket (intrascleral implanting method) in medium-sized animal (rabbits). The aims of this study were threefold: to determine the safety of this surgical technique, to establish the threshold current to elicit electrically evoked cortical potentials (EEPs), and to determine the retinal damage induced by the electrodes and by the electrical currents.

Materials and methods

Six pigmented rabbits (weighing 1.9–2.2 kg) were initially anesthetized with an intramuscular injection of ketamine hydrochloride (50 mg/kg) and xylazine hydrochloride (5 mg/kg). This amount of anesthetic kept the rabbits under a surgical level of anesthesia for 3 h. One eye was dilated with 0.5% tropicamide and 0.5% phenylephrine hydrochloride.

The procedures used on all animals conformed to the Institutional Guidelines of Osaka University and the ARVO Resolution on the Use of Animals in Research.

Stimulating electrodes

A photograph of the surface of the electrode array displaying the configuration of the electrodes is shown in Fig. 1. Eight dome-shaped microelectrodes (fabricated by NIDEK Co., Gamagori, Japan) were mounted in a polyimide strip, and the array was 2 mm wide, 4 mm long, and 180 μm thick. The dimensions of each electrode were as follows: height above the surface, 120–130 μm; diameter, 250 μm. The distance between electrodes was 500 μm. The impedance of the electrodes in saline is 10 kΩ at 1 kHz. The electrode array was connected to an external stimulator unit with insulated copper wires. Each electrode was coated with gold and was able to be activated separately.

Surgical method

The rabbit's eye was proptosed from the eye socket and draped with sterile rubberized cloth. After cutting the inferior half of the conjunctiva around the limbus, and cutting the inferior rectus and the inferior oblique muscles, the bare sclera was exposed. A scleral pocket (3×5 mm) was created just over the area of the visual streak, which was about 12 mm posterior to the limbus.

The multichannel electrode array was then implanted into the scleral pocket and sutured with 5-0 Dacron onto the sclera just above the pocket. The bundle of insulated leads from the microarray was also sutured at the limbus with 5-0 Dacron (Fig. 2). The surgical procedures took about 30 min.

An electronic stimulator (SEN-7203, Nihon Kohden, Shinjyuku, Japan) was then connected through an isolator (A-395R, World Precision Instruments, Sarasota, FL, USA) to the microelectrode array. The reference electrode was a platinum (Pt) wire coated with polyurethane resin and exposed at the tip. It was inserted 4 mm into the vitreous cavity and was fixed 2 mm from the limbus with 5-0 Dacron sutures.

Fig. 1 Photograph of the electrode array. (*Scale bar* 1 mm). Eight gold electrodes (*a–h*) are mounted in a polyimide strip. Each electrode had the following dimension: height, 120–130 μm; diameter, 250 μm; impedance, 10 kΩ at 1 kHz. The distance between electrodes was 500 μm

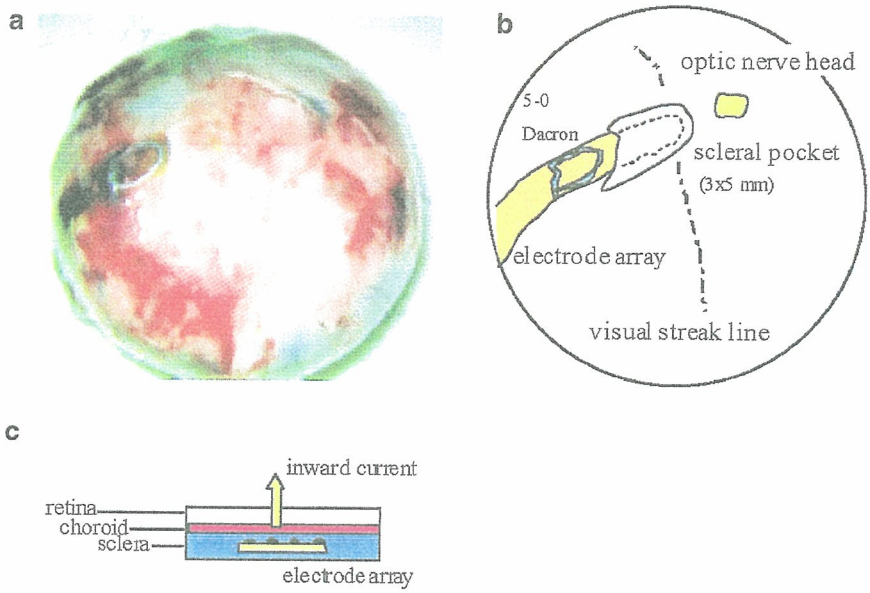

Fig. 2 **a** A photograph of an enucleated rabbit eye which has the microelectrode array implanted into the scleral pocket. **b** A schematic diagram of the electrode array that is inserted into a 3×5-mm scleral pocket over the visual streak. **c** A schematic diagram of transretinal electrical stimulation

Recording electrode

After exposing the skull, a stainless steel recording electrode was screwed into the skull bone above the visual cortex. The position of the electrode was 8 mm rostral to the lambda suture and 7 mm lateral to the midline [1, 8]. The reference needle stainless steel electrode was then placed between the skin and skull near the ear.

To confirm that the recording electrode was placed over the visual cortex, visual evoked potentials (VEPs) elicited by photic stimuli (1.2 J, 15 cm from the cornea) were recorded. The EEPs were elicited by monophasic electrical pulses of 0.5 ms duration, and 50 responses were averaged. A bandpass filter of 5 Hz to 1 kHz was used.

Electrical threshold current

The electric current was changed from 10 μA to 700 μA, and the direction of the current was first set for inward-flowing currents (electrode array positive and reference electrode negative), then the polarity was reversed for outward-flowing currents (electrode array negative and reference electrode positive).

For the purpose of finding the threshold current, the amplitudes of the EEPs elicited by a current of 500 μA delivered by each of the eight electrodes were compared. The electrode which elicited the largest EEP was selected to determine the threshold current. With this electrode, the electric current was decreased in steps, and the minimum electric current that elicited the first or second positive peak of the EEP (P_1 or P_2) was defined as the threshold current. The threshold current was also determined by reversing the polarity of the stimulating current.

Histology

At the completion of the experiment, the rabbit was killed by an overdose of barbiturate (100 mg/kg), and the eye was enucleated for histological examination. The eyes were embedded in paraffin, and 10-μm sections were cut and stained with hematoxylin and eosin (HE staining). Light microscopy was used to evaluate tissue damage. The electrode array used for stimulation was examined after the experiment with a scanning electron microscope.

Results

The electrode arrays were inserted and positioned without complications, and the placement of the recording electrode into the rabbit's skull was also completed without complications. Although the overall experiment time was only 3–4 h, early adverse effects were not detected in the eyes and brains surrounding the stimulating and recording electrodes.

The VEPs consisted of three large positive waves (Fig. 3a). The mean implicit time of the first positive peak (P_{v1}) was 23.8±1.2 ms, the second peak (P_{v2}) was 41.0± 3.0 ms, and the third peak (P_{v3}) was 58.2±2.1 ms (mean± SEM; n=6).

EEPs were also recorded in all rabbits. The mean implicit times of the EEP with an inward current (amplitude 500 μA; duration 0.5 ms) were 15.7±2.0 ms for P_{i1}, 27.3± 0.6 ms for P_{i2}, and 41.2±0.9 ms for P_{i3} (Fig. 3b). The implicit time of P_{i1} was significantly shorter than that for P_{v1}.

The waveform of EEPs with outward current with the same stimulus parameters consisted of four peaks, which were slightly different from that evoked by inward currents. The implicit times were 19.3±0.7 ms for P_{o1}, 30.1±

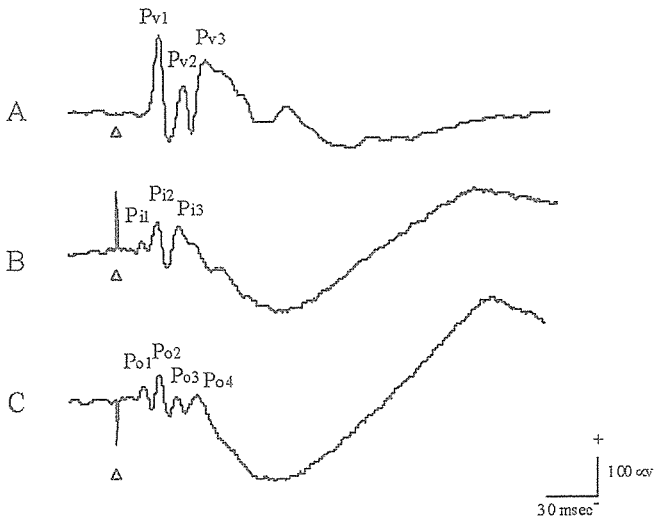

Fig. 3 Typical waveforms of VEP and EEPs. a VEP consists of three large positive components. The first positive peak (P_{v1}) had an implicit time of 24 ms, the second positive peak (P_{v2}) had an implicit time of 41 ms, and the third positive peak (P_{v3}) had an implicit time of 58 ms. b EEP with inward current (sclera+/vitreous−) shows an upward artifact at the onset of the stimulation. The first positive peak (P_{i1}) had an implicit time of 16 ms, a second positive peak (P_{i2}) had an implicit time of 27 ms, and a third positive peak (P_{i3}) had an implicit time of 41 ms. c EEP with outward current (sclera−/vitreous +) shows a negative downward artifact at the time of stimulation. The first positive peak (P_{o1}) had an implicit time of 19 ms, the second positive peak (P_{o2}) had an implicit time of 30 ms, a third positive peak (P_{o3}) had an implicit time of 42 ms, and a fourth positive peak (P_{o4}) had an implicit time of 59 ms

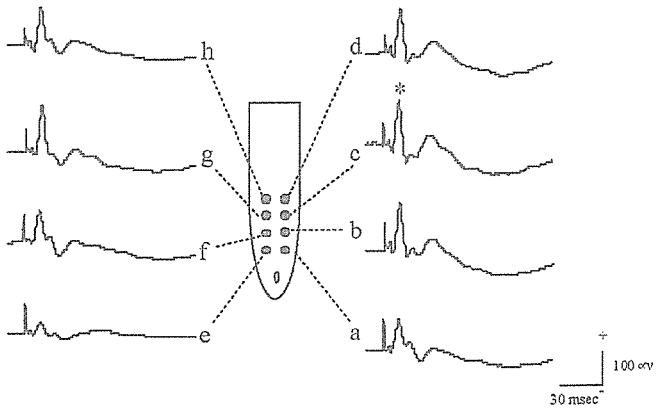

Fig. 4 EEPs elicited by inward electrical pulses from each of the eight electrodes. The amplitude of second positive peak (P_2) varies with the different electrodes. Because electrode *c* elicited the largest amplitude (*), electrode *c* was used for determining the threshold electrical current

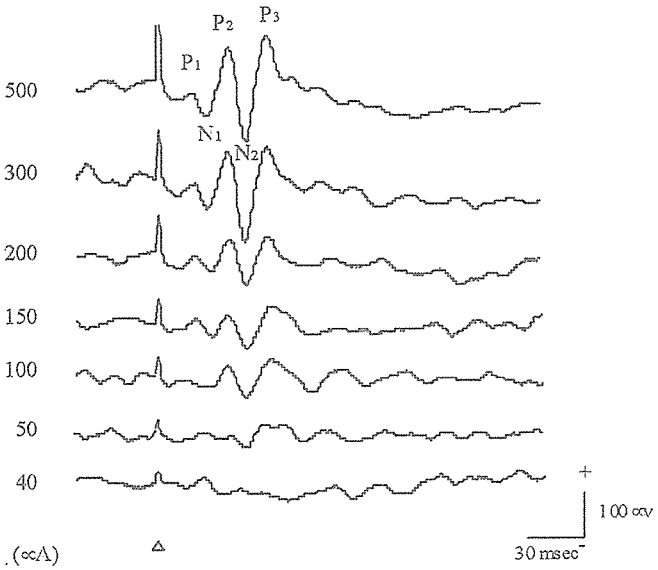

Fig. 5 Changes of the EEP waveforms with decreasing inward electrical currents for stimulation. The second and third positive peaks (P_2, P_3) were detectable with stimulus intensity ≤50 μA. The negative peaks (N_1, N_2) were detectable with stimulus intensity ≤100 μA

0.8 ms for P_{o2}, 41.6±0.9 ms for P_{o3}, and 59.0±0.7 ms for P_{o4} (Fig. 3c). The implicit times of P_{o1} and P_{o2} were slightly longer than P_{i1} and P_{i2}, but that of P_{o3} was not significantly different from that of P_{i3}.

The mean amplitude of the EEPs elicited by 500 μA inward current was 190±26 μV, while that for 500 μA outward current was 150±22 μV (n=6). Because the inward current elicited significantly larger EEPs, we selected the inward current for determining the thresholds.

The EEPs elicited by stimulating with each of the eight electrodes are compared in Fig. 4. Although the overall shape was similar for each of the electrodes, the peak amplitude of the second positive component (P_2) was different. The largest amplitude was elicited by stimulating with electrode c, and it was used for determining the threshold currents.

The EEPs elicited with decreasing inward currents are shown in Fig. 5. For the second (P_2) and third (P_3) peaks, the minimum stimulation current to elicit these peaks was obtained with 50 μA. For the negative components, the first negative peak (N_1) and the second negative peak (N_2) were obtained until 100 μA. The mean threshold current that elicited a small EEP was 55.0±10.0 μA for the six rabbits (27.5±5.0 nC).

The relationship between the averaged peak-to-peak amplitude (P_2 to N_2) of the EEPs and the inward current was examined in the six rabbits (Fig. 6). The regression curve showed that the EEP amplitude increased almost linearly with the lower stimulus currents and tended to be saturated with higher stimulus currents.

Histology

Examination of the histological sections surrounding the implanted electrode showed no obvious damage to the retina, choroid, and sclera at the light-microscopic level. Although a fissure was observed in the sclera which cor-

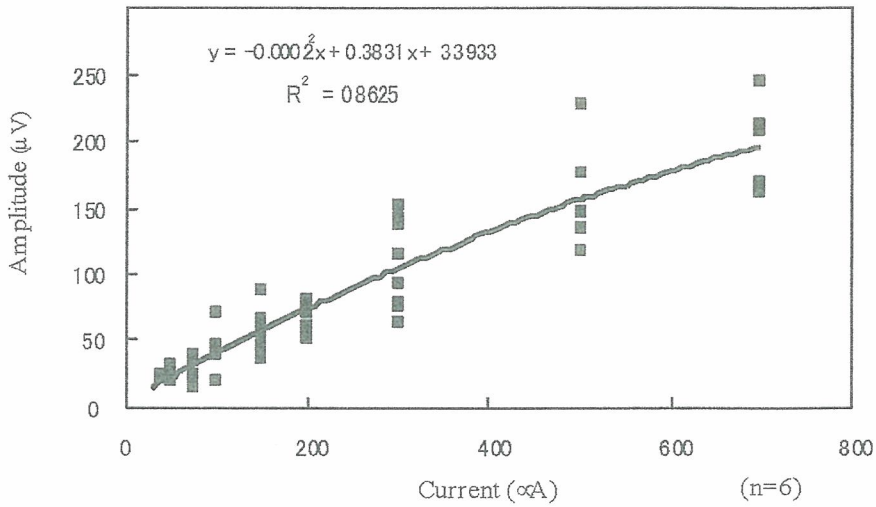

Fig. 6 Averaged peak-to-peak (from P_2 to N_2) amplitude (ordinate) of retinal response elicited by increasing inward current stimulation (*abscissa*). The regression curve shows a slow increase of EEP amplitude with stimulus current amplitude. The increase in the response amplitude is approximately linear with low stimulus current and tended to be saturated with greater stimulus currents

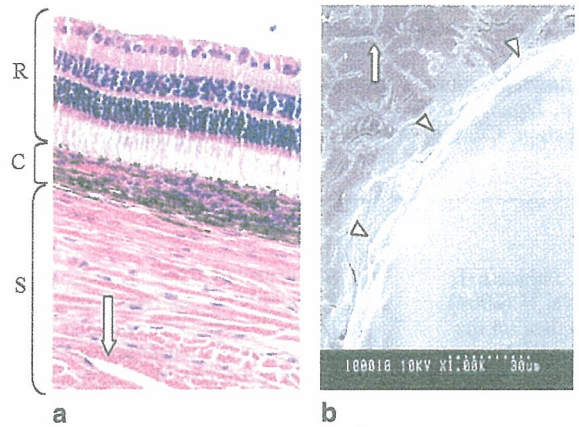

Fig. 7 **a** Histology of the retina and sclera around the electrode. The retina shows no significant damage around the area attached to the array. Degeneration and vacuolization cannot be seen in the sclera and retina. The *arrow* shows the edge of the scleral pocket. *R* Retina, *C* choroids, *S* sclera. HE staining, ×200. **b** A photograph of electrode array surface by scanning electron microscopy. The *arrowheads* point to the electrode surface. There is no deterioration such as cracks on the electrode, only dried crystals (*arrow*) of tissue fluids beside the electrode

responded with the scleral pocket, no significant tissue damage was observed in the sclera (Fig. 7a).

Scanning electron microscopic examination of the electrode also showed no evidence of electrode deterioration such as cracks on the electrode surface but only dried crystals of tissue fluids beside the electrode (Fig. 7b).

Discussion

In this study, we implanted a multichannel electrode array into the sclera. The implantation of electrodes intrasclerally was not difficult, and neither retinal hemorrhage nor retinal detachment was observed during or after the surgery, which suggests the safety of the surgical procedures.

The rabbit retina could be stimulated by STS using electrical currents from multichannel electrodes. The threshold charge for eliciting EEP was 27.5 nC, which is equivalent to a charge density of 56.0 μC/cm^2. Humayun et al. reported that a charge density of 8.92–11.9 μC/cm^2 was required to elicit EEPs from rabbits with epiretinal electrodes [6]. In experiments on cats, Dawson and Radtke found a threshold charge density of 30.5 μC/cm^2 [4]. Chow and Chow implanted their electrodes subretinally in rabbits and reported a threshold charge density of 2.8 nC/cm^2 to elicit EEPs [2]. Although the distance from the electrodes to the retina was farther for our transscleral electrodes than for epi- or subretinal electrodes, the threshold charge density to elicit EEPs was comparable with the other electrode placements.

After changing the polarity to outward currents, the mean threshold was elevated to 75.0 μA (37.5 nC), which was higher than that for inward currents. This finding is consistent with our previous reports that the threshold of inward currents was lower than that of outward currents to elicit EEPs in rats [9].

McCreery et al. reported that the electric charge which can elicit EEPs without damaging the neural tissue was 50 nC or an electrical charge density of 10 μC/cm^2 [12]. This is thought to be the borderline for chronic clinical stimulation; thus, it was recommended that the stimulating electrical current be kept below this charge density. For our system, the electrical charge current was at the upper limit of this borderline, but the charge density exceeded the borderline. Our stimulation method was not a direct stimulation of neural tissue, but an indirect transretinal stimulation. Therefore, the limit of electrical charge density may be expected to be higher than that with direct retinal stimulation.

The retinal origin of EEPs evoked by STS is still unknown. Our previous report [9] showed that STS elicited EEPs without photoreceptors in RCS rat, suggesting that

STS can stimulate the inner retinal neurons. In this study, paying attention to the implicit time of the first EEP peak (P_1) was shorter than that of the first VEP peak (P_{v1}), which suggested that the neuronal processes underlying EEPs by our method were faster than those involved in light stimulation. This shorter implicit time suggests again that STS had elicited EEP by stimulating the inner layers of normal rabbit retina.

The EEP waveforms elicited by intrascleral stimulation were similar to the EEPs elicited by subretinal stimulation [2, 14] or by epiretinal stimulation [13, 16]. They all had several fast wavelets followed by a large slow wave with a latency around 100 ms. Thus, we conclude that we can stimulate the same neural components by intrascleral transretinal stimulation as by epi- or subretinal stimulation.

Our histopathological examinations showed that no obvious damage occurred at the light-microscopic level in the retinal and scleral tissues with the electrical currents used in these acute experiments. Scanning electron microscopy showed no deterioration such as cracks on the used electrode surface. These results showed that the threshold of electric current was low enough to preserve the retinal tissue, and that our stimulating method was also safe.

Although some researchers have reported that the epiretinal [15] and subretinal [3] methods are safe for the retinal tissue, subretinal implantation can cause damage to the outer segments of photoreceptors [14] and induce glial proliferation when chronically implanted [17]. Epiretinal implantation can cause damage around the area of the retinal plug [10, 15], or may be unstable without the use of special devices to fix the electrodes [18]. Our method, on the other hand, requires only scleral surgery and there is no direct invasion of retinal tissue. This simplicity makes the intrascleral electrode insertion a safe and promising method.

In conclusion, our novel surgical procedure, an intrascleral implantation method for STS, represents a safe method for implanting an electrode array in rabbit eyes. EEPs were elicited from the visual cortex with a low electrical current, and the tissue damage was minimal around the electrode. In the future, this method has a potential of increasing the number of electrodes. However, additional studies are necessary to determine the spatial resolution and the long-term effects on the surrounding tissues.

Acknowledgements This study was supported by Health Science Grant, Japan, and by a grant (No. 14571670) from the Ministry of Education, Culture, Sports, Science and Technology, Japan.

References

1. Choudhury DP (1978) Visual field representation in the newborn rabbit's cortex. Brain Res 153:27–37
2. Chow AY, Chow VY (1997) Subretinal electrical stimulation of the rabbit retina. Neurosci Lett 225:13–16
3. Chow AY, Pardue MT, Perlman JI, Ball SL, Chow VY, Helting JR, Peyman GA, Liang C, Stubbs EB Jr, Peachey NS (2002) Subretinal implantation of semiconductor-based photodiodes: durability of novel implant designs. J Rehabil Res Dev 39:313–322
4. Dawson WW, Radtke ND (1977) The electrical stimulation of the retina by indwelling electrodes. Invest Ophthalmol Vis Sci 16:249–252
5. Eckmiller R (1997) Learning retina implants with epiretinal contacts. Ophthalmic Res 29:281–289
6. Humayun MS, Probst R, de Juan E Jr, McCormick K, Hickingbotham D (1994) Bipolar surface electrical stimulation of the vertebrate retina. Arch Ophthalmol 114:40–46
7. Humayun MS (2001) Intraocular retinal prosthesis. Trans Am Ophthalmol Soc 99:271–300
8. Inoue J, Potts AM (1971) Electrically evoked response of the visual system (EER) in the rabbit. Nippon Ganka Gakkai Zasshi 20(75):765–772
9. Kanda H, Morimoto T, Fujikado T, Tano Y, Fukuda Y, Sawai H (2004) Electrophysiological studies on the feasibility of suprachoroidal–transretinal stimulation for artificial vision in normal and RCS rats. Invest Ophthalmol Vis Sci 45:560–566
10. Majji AB, Humayun MS, Weiland JD, Suzuki S, D'anna SA, de Juan E Jr (1999) Long-term histological and electrophysiological results of an inactive epiretinal electrode array implantation in dogs. Invest Ophthalmol Vis Sci 40:2073–2081
11. Margalit E, Maia M, Weiland JD, Greenberg RJ, Fujii GY, Torres G, Piyathaisere DV, O'Hearn TM, Liu W, Lazzi G, Dagnelie G, Scribner DA, de Juan E Jr, Humayun MS (2002) Retinal prosthesis for the blind. Surv Ophthalmol 47:335–356
12. McCreery DB, Agnew WF, Yuen TG, Bullara L (1990) Charge density and charge per phase as cofactors in neural injury induced by electrical stimulation. IEEE Trans Biomed Eng 37:996–1001
13. Nadig MN (1999) Development of a silicon retinal implant: cortical evoked potentials following focal stimulation of the rabbit retina with light and electricity. Clin Neurophysiol 110:1545–1553
14. Schwahn HN, Gekeler F, Kohler K, Kobuch K, Sachs HG, Schulmeyer F, Jakob W, Gabel VP, Zrenner E (2001) Studies on the feasibility of a subretinal visual prosthesis: data from Yucatan micropig and rabbit. Graefes Arch Clin Exp Ophthalmol 239:961–967
15. Walter P, Szurman P, Viobig M, Berk H, Ludtke-Handjery H-C, Deng HR, Mittermayer C, Heimann K, Sellhaus B (1999) Successful long term implantation of electrically inactive epiretinal microelectrode arrays in rabbits. Retina 19:546–552
16. Walter P, Heimann K (2000) Evoked cortical potential after electrical stimulation of the inner retina in rabbits. Graefes Arch Clin Exp Ophthalmol 238:315–318
17. Zrenner E, Stett A, Weiss S, Aramant RB, Guenther E, Kohler K, Miliczek KD, Seiler MJ, Haemmerle H (1999) Can subretinal microphotodiodes successfully replace degenerated photoreceptors? Vision Res 39:2555–2567
18. Zrenner E (2002) Will retinal implants restore vision? Science 295:1022–1025

Transcorneal Electrical Stimulation Rescues Axotomized Retinal Ganglion Cells by Activating Endogenous Retinal IGF-1 System

Takeshi Morimoto,[1,2,3] Tomomitsu Miyoshi,[1] Satoshi Matsuda,[3] Yasuo Tano,[3] Takashi Fujikado,[2,3] and Yutaka Fukuda[1]

PURPOSE. To investigate the effect of transcorneal electrical stimulation (TES) on the survival of axotomized RGCs and the mechanism underlying the TES-induced neuroprotection in vivo.

METHODS. Adult male Wistar rats received TES after optic nerve (ON) transection. Seven days after the ON transection, the density of the surviving RGCs was determined, to evaluate the neuroprotective effect of TES. The levels of the mRNA and protein of insulin-like growth factor (IGF)-1 in the retina after TES were determined by RT-PCR and Northern and Western blot analyses. The localization of IGF-1 protein in the retina was examined by immunohistochemistry.

RESULTS. TES after ON transection increased the survival of axotomized RGCs in vivo, and the degree of rescue depended on the strength of the electric charge. RT-PCR and Northern and Western blot analyses revealed a gradual upregulation of intrinsic IGF-1 in the retina after TES. Immunohistochemical analysis showed that IGF-1 immunoreactivity was localized initially in the endfeet of Müller cells and then diffused into the inner retina.

CONCLUSIONS. TES can rescue the axotomized RGCs by increasing the level of IGF-1 production by Müller cells. These findings provide a new therapeutic approach to prevent or delay the degeneration of retinal neurons without the administration of exogenous neurotrophic factors. (*Invest Ophthalmol Vis Sci.* 2005;46:2147–2155) DOI:10.1167/iovs.04-1339

Injury to retinal ganglion cells (RGCs) causes functional loss of vision that is irreversible because of the limited axonal regeneration of RGCs.[1] Although much research has been performed on the effect of injuries to neurons of the central nervous system (CNS) and on potential therapeutic strategies to promote axonal regeneration, a complete functional recovery has not been achieved and remains a major goal of this area of research.[2]

Axotomy of RGCs has been widely used as an experimental method to investigate whether different agents can protect the RGCs from apoptosis. In rats, axotomy of the RGCs by optic nerve (ON) transection induces apoptosis and results in rapid loss (within 2 weeks) of 85% of the RGC population.[3,4] To protect RGCs from this death, many attempts have been made to administer drugs or genes expressing various neurotrophic factors.[5–11] These trials, however, have had limited success, and many obstacles and negative side effects have arisen that have prevent widespread clinical application of these methods. Thus, it is necessary to devise other treatments using new therapeutic strategies to find a better method to protect damaged RGCs.

Recently, we discovered that direct electrical stimulation of the transected ON increases the survival of axotomized RGCs in vivo.[12] The protective effect of ON electrical stimulation (ONES) suggests that electrical stimulation of neural tissues may be a strategic approach to treat injured axons in the visual pathway. ONES is, however, too invasive to be clinically applicable, and so we tried transcorneal electrical stimulation (TES), which is known to activate inner retinal neurons and to evoke light sensations or phosphenes, in human[13] and animal[14,15] eyes. Its neuroprotective effect, however, has not been examined.

The purpose of this study was to evaluate the effect of TES on the survival of axotomized RGCs in vivo and to determine the mechanism of how TES protects axotomized RGCs. Because it has been reported that the expression of neurotrophic factors can be altered by electrical or physiological stimuli in vivo,[16–19] we hypothesized that TES upregulates some neurotrophic factors and/or their receptors in the retina. The results show that the level of insulin-like growth factor (IGF)-1 increased in the retina after TES and identified Müller cells as the source of IGF-1.

MATERIALS AND METHODS

Experimental Animals

Adult male Wistar rats (230–270 g) were obtained from SLC Japan, Inc. (Shizuoka, Japan). All experimental procedures were performed in accordance with the ARVO Statement for the Use of Animals in Ophthalmic and Vision Research and were approved by the Animal Research Committee, Osaka University Medical School. The animals were anesthetized with intraperitoneal pentobarbital (50 mg/kg body weight) for all surgical procedures.

Retrograde Labeling of RGCs

To identify RGCs from other retinal cells, they were retrogradely labeled with a fluorescent tracer (Fluorogold [FG]; Fluorochrome Inc., Englewood, CO). A small sponge soaked in 2% FG (in 0.9% NaCl containing 10% dimethyl sulfoxide) was placed on the surface of both superior colliculi after opening the skull dorsal to the lambda fissure.[3,7,12]

From the Departments of [1]Physiology and Biosignaling, [2]Visual Science, and [3]Ophthalmology, Osaka University Medical School, Osaka, Japan.

Supported by Grants-in-Aid for Scientific Research (TMo, TMi, YT, TF); Health Sciences Research Grant from the Ministry of Health, Labour and Welfare, Japan (YT, YF, TF); and the Marine and Fire Insurance Association of Japan (TMi); TMo is a recipient of Research Fellowship of the Japan Society for the Promotion of Science for Young Scientists.

Submitted for publication November 17, 2004; revised January 31, 2005; accepted February 14, 2005.

Disclosure: **T. Morimoto**, None; **T. Miyoshi**, None; **S. Matsuda**, None; **Y. Tano**, None; **T. Fujikado**, None; **Y. Fukuda**, None

The publication costs of this article were defrayed in part by page charge payment. This article must therefore be marked "*advertisement*" in accordance with 18 U.S.C. §1734 solely to indicate this fact.

Corresponding author: Tomomitsu Miyoshi, Department of Physiology and Biosignaling, Osaka University Medical School, 2-2 Yamadaoka, Suita City, Osaka 565-0871, Japan;
tmiyoshi@phys2.med.osaka-u.ac.jp.

ON Transection

Seven days after retrograde labeling, the left ON was transected as described in detail elsewhere.[3,4,12] Briefly, a skin incision was made through the left eyelid close to the superior orbital rim, and the orbit was opened. After the superior extraocular muscles were spread, the ON was exposed by a longitudinal incision of the orbital retractor muscle and perineurium. The ON was transected approximately 3 mm from the posterior pole of the eye, with care taken not to damage the retinal blood circulation.

Transcorneal Electrical Stimulation

For electrical stimulation, a noninvasive bipolar contact lens electrode with an inner and outer ring that served as the stimulating electrodes (Kyoto Contact, Kyoto, Japan) was used. Under corneal surface anesthesia by 0.4% oxybuprocaine HCl in addition to systemic anesthesia, the contact lens electrode was placed on the cornea of the eye in which the ON had been transected. Hydroxyethylcellulose gel (1.3%) was applied for corneal protection and for tight adhesion of the electrode to the cornea.

The electrical stimuli consisted of 20 Hz, biphasic rectangular current pulses (100 μA) that were delivered from an isolated constant-current stimulator (Stimulator, SEN-7203; Nihon Kohden, Tokyo, Japan; Isolator, A395R; World Precision Instruments, Sarasota, FL). The electrical stimulation lasted for 1 hour. To evaluate the neuroprotective effect of TES, the pulse duration of electric current was varied from 0 (sham stimulation) to 3 ms/phase. TES was commenced immediately after ON transection.

Quantification of RGC Density

Seven days after ON transection, rats received an overdose of pentobarbital and were perfused transcardially with saline followed by 4% paraformaldehyde (PFA) in 0.1 M phosphate buffer (PB). Both eyes were enucleated, and the retinas were isolated and flatmounted on glass slides. The retinas were examined under a fluorescence microscope (Axioskop; Carl Zeiss, Oberkochen, Germany) with a UV filter (365 nm). The number of FG-labeled neurons was counted in 12 areas (0.5 mm^2 each) at distances of 1, 2, and 3 mm from the optic disc along the nasotemporal and dorsoventral midlines (upper, lower, nasal, and temporal direction). The density of surviving RGCs was calculated from the number of FG-labeled neurons counted in the 12 areas. The data are reported as the mean ± standard deviation.

The statistical significance of differences was determined by one-way ANOVA followed by the Tukey test. Statistical significance was set at $P < 0.05$.

RNA Extraction, RT-PCR, and Northern Blot Analysis

Eyes without ON transection underwent TES for 1 hour, and were removed at different selected time points from 1 hour to 10 days. The retinas were dissected from the eyes in a shallow bath of cold phosphate buffered saline (PBS) and were stored at −80°C until use. Total RNA was then extracted (RNeasy Mini Kit; Qiagen, Hilden, Germany) from pooled retinas and quantified (Gene Quant II; Amersham Pharmacia Biotech, Piscataway, NJ), as previously described.[20]

RT-PCR and Northern blot analysis were performed as previously described.[21] For RT-PCR, 5 μg of total RNA was reverse transcribed using oligo (dT) reverse transcriptase (Ready-To-Go You-Prime First-Strand Beads; Amersham Biosciences). The cDNAs were amplified for 25 to 30 cycles of 30 seconds at 95°C, 30 seconds at 55°C, and 60 seconds at 72°C. The sequences of the primers used were: IGF-1 forward, 5′-TGGACGCTCTTCAGTTCGTG-3′, reverse, 5′-GTTTCCTG-CACTTCCTCTAC-3′; IGF-1R forward, 5′-CAGCTGCAACCACGAGG-CTG-3′, reverse, 5′-GGTTCACAGAGGCGTACAGC-3′; BDNF forward, 5′-AGAGCTGCTGGATGAGGACC-3′, reverse, 5′-CCAGTGCCTTTTGTC-TATCG-3′; TrkB forward, 5′-CTTGGAGAAGGAGCCTTTGG-3′, reverse, 5′-CAACCCGGTAGTAGTCGGTG-3′; bFGF forward, 5′-CGGCAGCAT-CACTTCGCTTC-3′, reverse, 5′-CAGTATGGCCTTCTGTCCAG-3′; FGFR-1 forward, 5′-ACCTGATCTCGGAGATGGAG-3′, reverse, 5′-TGGTGGGT-GTAGATCCGGTC-3′; CNTF forward, 5′-TGAGGCAGAGCGACTCCA-AG-3′, reverse, 5′-GCTCTCAAGTGCTGAGATTC-3′; CNTFR forward, 5′-TTGGGTCACAACACCACGGC-3′, reverse, 5′-CCAAGGAGCTGGTG-GTGCTG-3′; and β-actin forward, 5′-TGCCCATCTATGAGGGTTA-CG-3′, reverse, 5′-TAGAAGCATTTGCGGTGCGGTGCACG-3′.

For Northern blot analysis, total RNA (10 μg) was isolated from the retina at each time point by electrophoresis on 1.0% agarose-formaldehyde gels and transferred overnight onto polyvinylidene difluoride (PVDF) membranes (Millipore Corp., Bedford, MA). The membrane was prehybridized for 1 hour at 65°C in hybridization buffer (0.9 M NaCl, 90 mM sodium citrate [pH 7.0]) containing 5× Denhardt's solution, SDS (0.5%), and heat-denatured salmon sperm DNA (100 ng/mL). The cDNA probe was radiolabeled with [32P]dCTP (NZ522; PerkinElmer Life and Analytical Sciences, Boston, MA, with the Random Primer DNA Labeling Kit, ver. 2; Takara Bio, Shiga, Japan). After hybridization overnight at 65°C in hybridization buffer containing radiolabeled cDNA probe (5 ng/mL), filters were washed twice with 2× SSC, 0.5% SDS and 0.2× SSC, 0.5% SDS for 60 minutes at 65°C, exposed to x-ray film (Fuji Film, Kanagawa, Japan), and subjected to autoradiography. Autoradiograms were quantified by image analysis (Scion Image; Scion Corp., Frederick, MD). The relative expression levels of IGF-1 mRNA in the retinas after TES were compared with the expression in the control retina, which was normalized to 1.0. Data from three independent experiments are given as the mean ± SD.

Western Blot Analysis

Total retinal proteins were extracted from eyes at each time point after TES and were assessed by Western blot analysis, as previously described.[22,23] Total protein was extracted with lysis buffer (50 mM Tris-HCl [pH 7.4]); 0.5% deoxycholate, 1% Triton X-100, 1% NP-40, 10 mM NaF, 150 mM NaCl, 20 μg/mL aprotinin, 20 μg/mL leupeptin, 20 μg/mL pepstatin, 0.5 mM phenylmethylsulfonyl fluoride [PMSF], 1 mM Na_3VO_4, 1 mM dithiothreitol, and 10% SDS) on ice for 30 minutes and centrifuged at 15,000 rpm for 15 minutes at 4°C. The supernatants were collected, and the protein concentration was determined by the Bradford protein assay with bovine serum albumin as a standard (Bio-Rad, Hercules, CA). Total protein (10 μg) was separated by SDS-PAGE (16% Tris-tricine gel; Invitrogen, Carlsbad, CA) and transferred to a PVDF membrane (Millipore Corp.).

Membranes were preblocked in 5% nonfat milk at room temperature (RT) for 1 hour and then incubated with primary antibodies of mouse anti-human IGF-1 (Upstate Biotechnology, Waltham, MA) at a dilution of 1:1000 in TBS and 0.1% Tween 20 (TBS-T) with 5% nonfat milk at 4°C overnight. Membranes were washed in TBS-T and incubated with HRP-conjugated goat IgG secondary antibody against mouse (Jackson ImmunoResearch, West Grove, PA; 1:1000 dilution in TBS-T with 5% nonfat milk) at RT for 1 hour. Labeled proteins were detected by chemiluminescence (ECL; Amersham, Arlington Heights, IL), and the chemiluminescence signals were captured on film (Kodak scientific imaging film; Eastman Kodak, Rochester, NY). Densitometric analyses were then performed (Scion Image; Scion Corp.). First, the relative expression levels of IGF-1 protein were compared with the expression levels of β-actin in the same retinas. Then the values were compared with that of the control retina which was normalized to 1.0. The mean ± SD of three independent experiments was used for the analyses. Experiments for RT-PCR and Northern and Western blot analyses were performed on specimens collected from three animals at each time point, and the results were repeated three times.

Immunohistochemistry

On days 1, 4, 7, or 14 after TES without ON transection, the rats received an overdose of pentobarbital and were perfused transcardially with saline, followed by 4% PFA in 0.1 M PB and the eyes immediately

enucleated. The anterior segment and the lens were removed, and the remaining eyecup was immersed in the same fixative for 30 minutes at 4°C. The eyecups including the ON were cryoprotected in 10% to 20% sucrose in PBS for 2 days, embedded in OCT compound (Tissue-Tek; Ted Pella, Inc., Redding, CA) by snap freezing in liquid nitrogen, and then sectioned (10 μm). The sections were mounted on slides and incubated with blocking buffer (PBS containing 5% goat serum, 5% BSA, and 0.2% Triton X-100) at RT for 1 hour. After three washes in 0.1 M PBS, the sections were incubated overnight at 4°C with a mouse monoclonal antibody against IGF-1 (1:300 dilution; Upstate Biotechnology) and/or a rabbit polyclonal antibody against glutamine synthetase (1:300; Santa Cruz Biotechnology, Santa Cruz, CA) diluted in PBS containing 0.2% Triton X-100, 5% goat serum, and 5% BSA. The sections were then rinsed three times in 0.1 M PBS and incubated with Cy3- and fluorescein isothiocyanate (FITC)-conjugated goat IgG secondary antibodies (1:200; Jackson ImmunoResearch) at RT for 1 hour, followed by three rinses with 0.1 M PBS. The sections were mounted with antifade mounting medium (Vectashield; Vector Laboratories, Burlingame, CA) and examined with a confocal laser microscope (LSM510; Carl Zeiss Meditec).

Administration of IGF-1R Antagonist

JB-3, a selective antagonist for IGF-1R, is a cyclic D-amino acid peptide analogue of the D domain of IGF-1 (CYAAPSAYLKPC).[24,25] JB-3 was synthesized nonbiologically by Sigma Genosys Japan (Hokkaido, Japan). A subcutaneous injection of JB-3 has been shown to inhibit the activity of retinal IGF-1 action in a retinal neovascularization model.[24]

After ON transection, 200 μL of JB-3 solution was dissolved in 0.1 M PBS and was injected intraperitoneally every day for 1 week. For the control, PBS alone was injected. The dose of JB-3 was obtained from the protocol described by Smith et al.[24] This dosage schedule achieved a systemic dose of JB-3 of 10 μg/kg or 100 μg/kg per day, for 6 days.

Results

TES and the Survival of Axotomized RGCs In Vivo

Seven days after the retrograde labeling of the RGCs with FG, the left ON was transected, and TES was immediately applied for 1 hour. The rats were killed 7 days later, and the effect of the TES on the survival of axotomized RGCs was examined in flatmounts of the retina (Fig. 1). In intact control retinas, FG-labeled RGCs were recognized by the fine spots of fluorescence in the perinuclear cytoplasm and proximal dendrites (Fig. 1A). The mean RGC density in the intact control retinas was 2346 ± 175 cells/mm^2 (mean ± SD; $n = 12$; Fig. 2).

Seven days after ON transection and without TES, the number of FG-labeled RGCs was markedly reduced; they were irregularly shaped, and debris of dead RGCs were present (Fig. 1B). The mean RGC density had decreased to 54% of normal ($n = 8$).

The mean RGC density in the sham electrical stimulation was 53% ($n = 6$) of the control retinas. This reduction was not significantly different from that in the eyes with ON transection and without TES. In contrast, retinas that had received TES had many more surviving RGCs than those without electrical stimulation (Fig. 1C). The increase in the densities of RGCs depended on the pulse duration of electric current. TES of 0.5-ms/phase pulse duration significantly increased the number of RGCs (70% of the normal density; $n = 6$, $P < 0.05$). In addition, TES of 1- and 3-ms/phase pulse duration further increased the density up to 85% and 83%, respectively, of normal ($n = 6$, each; Fig. 2). The shapes of surviving RGCs were similar to those of the RGCs in the intact retinas. During the course of these experiments, cataracts or corneal opacities were not developed under surgical microscope in all rats. Fundus examination was performed at the end of TES, but neither retinal detachment nor vitreous hemorrhage occurred in all rats.

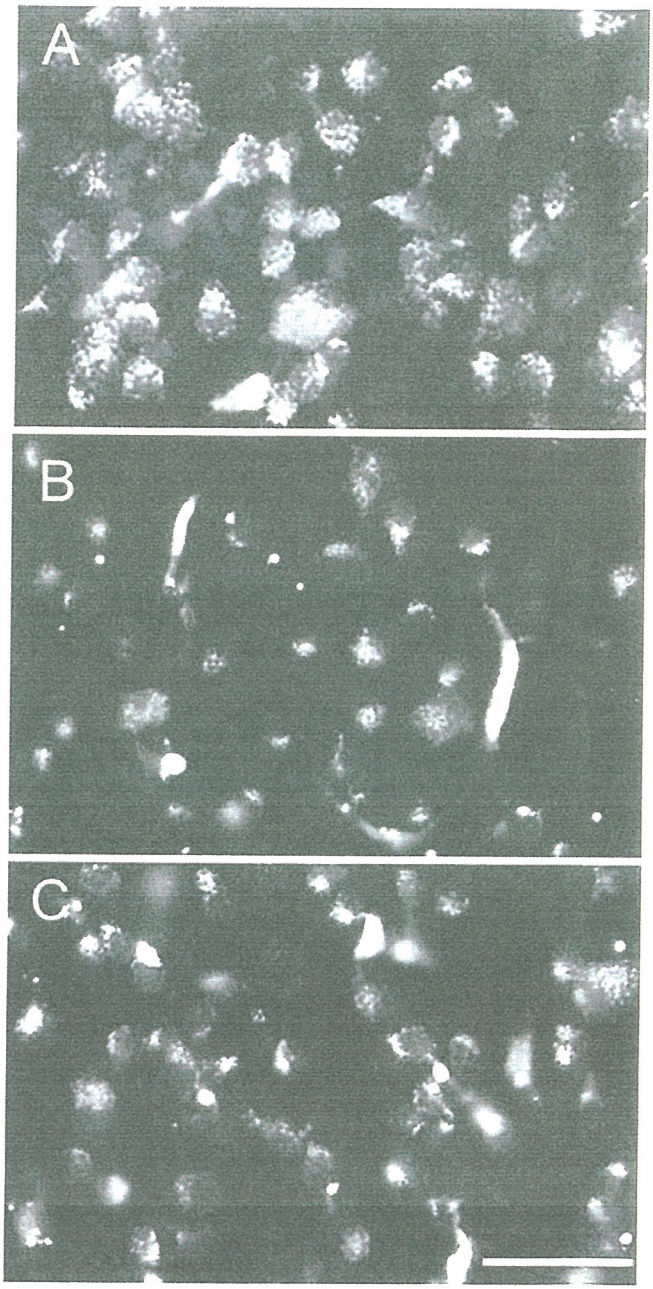

FIGURE 1. Representative photomicrographs of retrogradely-labeled RGCs in corresponding regions (approximately 1 mm from the optic disc) of flat-mounted retinas. (A) FG-labeled RGCs in intact control retina. (B) RGCs in the retina 7 days after ON transection without TES. (C) RGCs after ON transection with TES (1 ms/phase). More regularly shaped RGCs were seen in the retina after TES than in those without TES. Scale bar, 25 μm.

Increase in Level of IGF-1 after TES

We hypothesized that the neuroprotective effect of TES results from increasing the level of some neurotrophic factors or their receptors in the retina. To test this hypothesis, we examined which genes of the principal neurotrophic factors and their receptors were upregulated after TES (100 μA, 1 ms/phase, 20

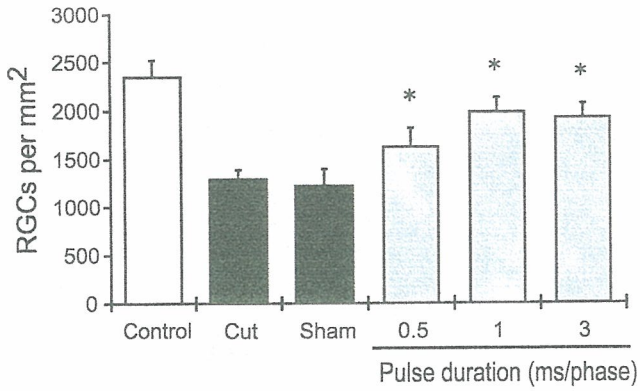

FIGURE 2. The neuroprotective effects of TES on the axotomized RGCs 7 days after ON transection depended on the pulse duration. The density of the FG-labeled RGCs per square millimeter is given as the mean ± SD. Seven days after ON transection, the density of the RGCs decreased to 54% of the control (Cut group). In the sham-treated animals (no electrical stimulation after ON transection), the density decreased to 53% of that of the intact control retina (Sham group). The RGC density in all three groups with TES (0.5, 1, and 3 ms/phase pulse duration) was significantly increased compared with that in the sham group. Statistical analysis was made by one-way ANOVA followed by the Tukey test ($P < 0.01$, $^*P < 0.05$ compared with sham).

Hz, 1 hour) without ON transection. RT-PCR was used to survey the changes in the mRNA expressions of the following neurotrophic factors and receptors: BDNF and its receptor TrkB; CNTF and CNTF receptor-α (CNTFRα); bFGF and FGF receptor-1 (FGFR-1); and IGF-1 and IGF-1 receptor (IGF-1R).

RT-PCR analysis showed that the expression level increased for only the mRNA of IGF-1, and the expression of the mRNA of the other neurotrophic factors and receptors did not change significantly (Fig. 3A). RT-PCR of IGF-1 mRNA also showed that its level of expression depended on the pulse duration of the TES (Fig. 3B). The expression of IGF-1 mRNA in the retina with 1-ms/phase pulses of TES was higher than that with 0.5-ms/phase on day 2 after TES, and this difference was maintained for at least 7 days.

A quantitative analysis of the changes of IGF-1 mRNA expression was also performed by Northern blot analysis at different times, ranging from 1 hour to 10 days after TES. Northern blot analysis showed that the level of mRNA of IGF-1 in the retina gradually increased from day 1 and reached a peak at day 7 (203% of the level of the intact control retina) and remained elevated even at day 10 after TES (Figs. 3C, 3D).

Western blot analysis was also used to determine the level of IGF-1 protein from day 1 to day 14. The level of IGF-1 protein was already increased on day 1 and reached its peak of 189% of the intact control on day 7. The elevated level was still present on day 10, confirming the results obtained from North-

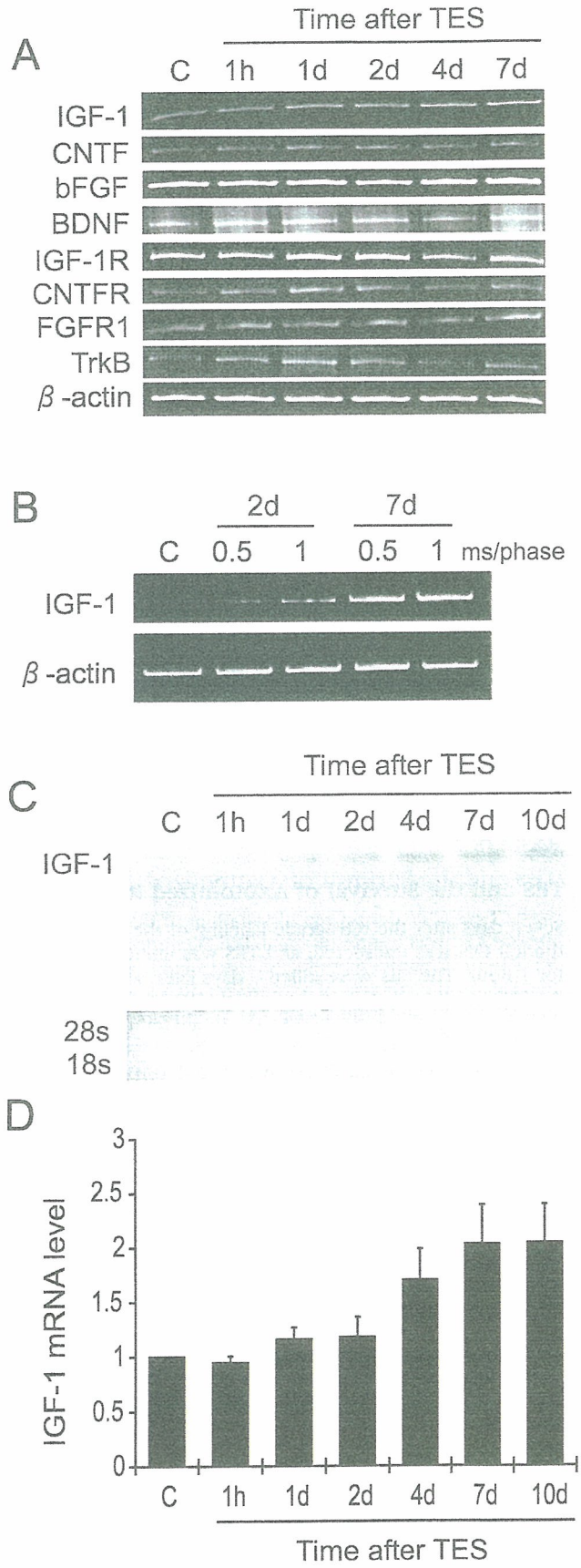

FIGURE 3. Expression of IGF-1 mRNA in the retina after TES. (A) RT-PCR analyses for four kinds of neurotrophic factors and receptors at different times ranging from 1 hour to 7 days after TES without ON transection. The data labeled "C" are from intact control retina. (B) Electrical current pulse duration-dependent upregulation of IGF-1 mRNA expression by RT-PCR analysis. RT-PCR for β-actin mRNA confirmed that equivalent amounts of RNA were used. (C) Northern blot analysis of IGF-1 mRNA in the retina (*top*). RNA loading was measured by gel staining with ethidium bromide (*bottom*). (D) Relative expression level of IGF-1 mRNA in retinas after TES compared with the control retinas (normalized to 1.0). The mean ± SD of data from three independent experiments is shown.

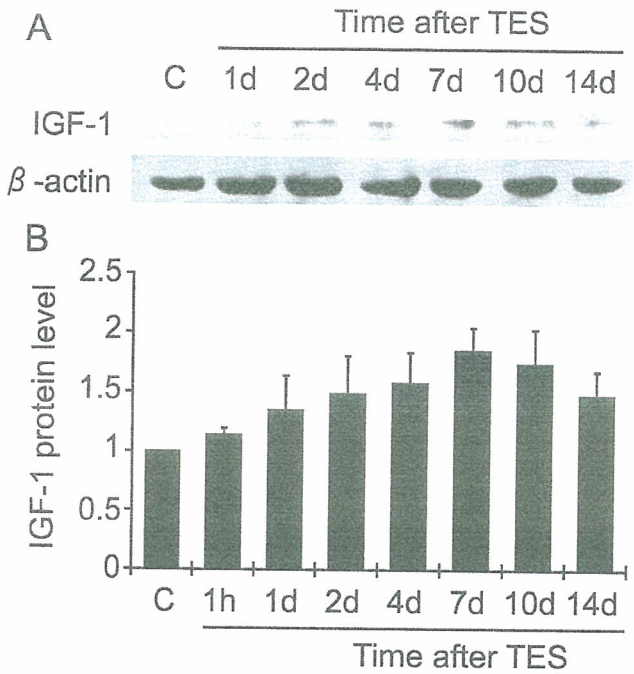

FIGURE 4. Expression of IGF-1 protein. (A) Western blot analysis of IGF-1 protein in the retina (*top*). (B) Relative expression of IGF-1 protein in retinas after TES compared with the contralateral control retinas (normalized to 1.0). Data from three independent experiments were averaged and are presented relative to that in the control retinas (mean ± SD).

ern blot analysis. However, the IGF-1 protein level then decreased on day 14 (Fig. 4).

Immunolocalization of IGF-1 in the Retina after TES

Immunohistochemical studies were performed with IGF-1 antibody, to determine the distribution of IGF-1 protein in the retina from day 1 to day 14 after TES without ON transection. In the intact control retina, IGF-1 immunoreactivity was very weak and restricted primarily to the inner limiting membrane (ILM) and the nerve fiber layer (NFL; Fig. 5A). On day 1 after TES, intense immunoreactivity for IGF-1 appeared from the ILM to the ganglion cell layer (GCL). A weak, but detectable, positive staining was also observed in the inner plexiform layer (IPL) and the inner nuclear layer (INL; Fig. 5B). On day 4, IGF-1 immunoreactivity further expanded, and the radial elements extending from the ILM to the IPL were stained (Fig. 5C). On day 7, the staining for IGF-1 was strongest within the inner retina, and intense staining for IGF-1 was seen in the radial processes of the ILM through the INL (Fig. 5D). On day 14, the immunoreactivity for IGF-1 in the inner retina decreased but IGF-1 signals in the radial processes remained within the NFL and GCL (Fig. 5E).

IGF-1 in Müller Cells

To determine whether Müller cells express IGF-1, additional immunohistochemical studies were performed on the retina with antibodies to IGF-1 and glutamine synthetase (GS), a specific marker for Müller cells. Müller cell bodies lie in a narrow band in the middle of the INL, and their processes span all cellular and plexiform layers of the retina.[26] The coimmunolocalization of IGF-1 (Fig. 5F) and GS (Fig. 5G) was not strong in the Müller cells of the intact retina. This indicates that IGF-1 was located mainly in the basal endfeet of the Müller cells in the intact retina (Fig. 5H). On day 7 after TES, IGF-1 immunoreactivity appeared in the Müller cell processes that extend from the ILM to the OLM and also in the space surrounding them within the IPL and INL (Figs. 5I–K). There was no difference in GS immunoreactivity between the control retina and the retina on day 7 after TES. Examination of the retinas at higher magnification on day 7 after TES showed that strong immunoreactivity of IGF-1 appeared in the endfeet of the Müller cells which surrounded the cells in the GCL (Fig. 5L–N).

We also performed immunohistochemical analysis for glial fibrillary acidic protein (GFAP) which is expressed in Müller cells whenever the retinal neurons are damaged.[27–30] We did not observe immunoreactivity for GFAP throughout the experimental period, suggesting that TES does not damage the retinal tissue (data are not shown). In agreement with the results from Western blot analysis, these results indicated that the IGF-1 is secreted from Müller cells and spreads throughout the inner retina and that TES increases the level of secretion.

Effect of Upregulation of IGF-1 on TES-Induced Neuroprotection of Axotomized RGCs

IGF-1 is one of the trophic factors that promote the survival of axotomized RGCs in vivo.[11] To determine whether IGF-1 is involved in the TES-induced neuroprotection, we counted the number of RGCs that survived after a combined treatment of TES and JB-3, an IGF-1 receptor antagonist.[24,25,31] JB-3 is a long-acting antagonistic peptide that inhibits interaction between IGF-1 and IGF-1R and prevents activation of tyrosine kinase of IGF-1R in a dose-dependent manner.[25,31] Daily injections of low-dose JB-3 (10 μg/kg per day) did not block the neuroprotective effects of TES, since the mean RGC density at day 7 after ON transection was 79% in the intact retina ($n = 4$), which was not significantly different from that after TES and PBS injection (86%; $n = 4$; Figs. 6A, 6B, 7).

However, a high dose of JB-3 (100 μg/kg per day) significantly inhibited the neuroprotective effects of TES, as the number of RGC was reduced to 59% of that in the control retina ($n = 4$; Figs. 6C, 7). With JB-3 alone, the number of surviving RGCs after ON transection (52%; $n = 4$), was similar to that with the ON transection without JB-3 ($n = 8$; Fig. 7). These data showed that the IGF-1 induced by TES plays a key role in TES-induced neuroprotection of axotomized RGCs.

DISCUSSION

Our results demonstrate that TES markedly increased the number of surviving axotomized RGCs in vivo, and the degree of protection was dependent on the strength of the electrical charge. Our results also show that the mRNA and protein of IGF-1 gradually increased in the retina during the 7 days after TES. Immunohistochemical analyses showed that the IGF-1 was located in the endfeet of the Müller cells, and TES led to a spread of IGF-1 in the intact retina. Thus, TES activated the Müller cells to produce more IGF-1 and release it into the inner retina. A blocking of the IGF-1R by JB-3 reduced the degree of neuroprotection by TES on the axotomized RGCs. Thus, TES activates an intrinsic retinal IGF-1 system that then rescues the axotomized RGCs.

IGF-1 as a Key Molecule for TES-Induced Neuroprotection

The upregulation of IGF-1 by the TES proved to be a crucial factor in neuroprotection. To the best of our knowledge, this is the first in vivo demonstration that a neurotrophic factor can be upregulated by electrical stimulation and can then lead to

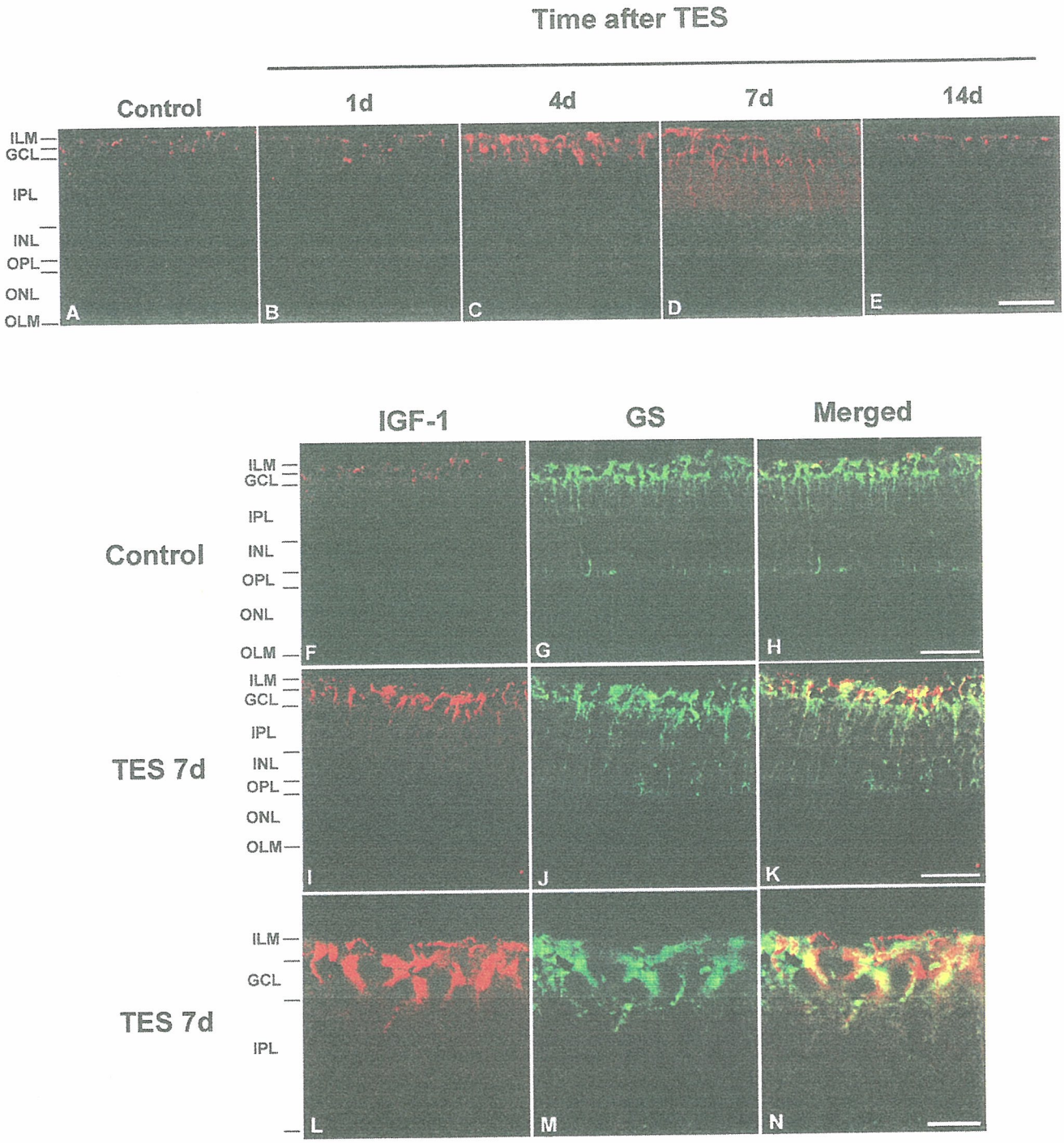

FIGURE 5. Immunohistochemical analysis of IGF-1 in the retina after TES. (**A–E**) Localization of IGF-1 in the retina at different time points after TES. IGF-1 immunoreactivity in the intact retina (**A**). IGF-1 staining increased on day 1 after TES (**B**) and increased more and spread from the ILM to the GCL 4 days after TES (**C**). IGF-1 immunoreactivity reached a peak on day 7 (**D**) and decreased on day 14 (**E**). (**F–N**) Double staining for IGF-1 (*red*) and GS (*green*), a specific marker of Müller cells in the retina. In the intact control retina, weak IGF-1 immunoreactivity was distributed from the ILM to the GCL (**F**), and GS immunoreactivity was present in Müller cells (**G**). The merged image (**H**) shows that weak signal (*yellow*) was localized in the ILM (**H**). Seven days after TES, strong immunoreactivity for IGF-1 appeared from the ILM to the IPL (**I**), and the merged image shows that IGF-1 immunoreactivity appeared in the endfeet and processes of Müller cells (**K**). A high-magnification view of IGF-1 and GS colocalization (**N**) strongly suggests that IGF-1 is produced in the endfeet of Müller cells surrounding the cells in GCL. Scale bars: (**A–E**) 100 μm; (**F–K**) 50 μm; (**L–N**) 20 μm.

neuroprotection. Until now, it has been reported that electrical or natural stimulation can modify the expression of neurotrophic factors or their receptors in neural tissue. Thus, electrical stimulation has been shown to upregulate BDNF and TrkB mRNA in various neurons.[16,17] The mRNA levels of BDNF or TrkB in the rat visual cortex were increased by light stimula-

tion.[18,19] In addition, it has been demonstrated that light-induced damage or mechanical injury to the retina elevates the expression of bFGF and CNTF.[27,28] Because various neurotrophic factors and their receptors are known to exist in the retina,[5,32–35] all of them can be upregulated in the retina by different types of stimuli. However, IGF-1 was specifically upregulated in the retina by TES.

We have shown an upregulation of IGF-1 by Northern and Western blot analyses and immunohistochemistry. We screened for BDNF, CNTF, and bFGF and their receptors in addition to IGF-1 and IGF-1R by RT-PCR, but other neurotrophic factors or receptors may also have contributed to the neuroprotective effects of TES. In addition to the possible upregulation of neurotrophic factors and/or receptors, TES can depolarize the RGCs directly. It has been reported that the neural activity of RGCs increases their sensitivity to peptidic neurotrophic factors.[36,37] We observed that TES of 100 μA at 1 ms/phase, which had been shown to rescue the axotomized RGCs, was also able to evoke electrical responses in the superior colliculus (data not shown). Thus, we cannot rule out the possibility that the electrical activation of the RGCs may have contributed to the effect of IGF-1. However, the systemic administration of JB-3 almost completely inhibited the TES-induced neuroprotection. This clearly shows that IGF-1 is essential for TES-induced neuroprotection, even though some other mechanisms may contribute to the effect of IGF-1.

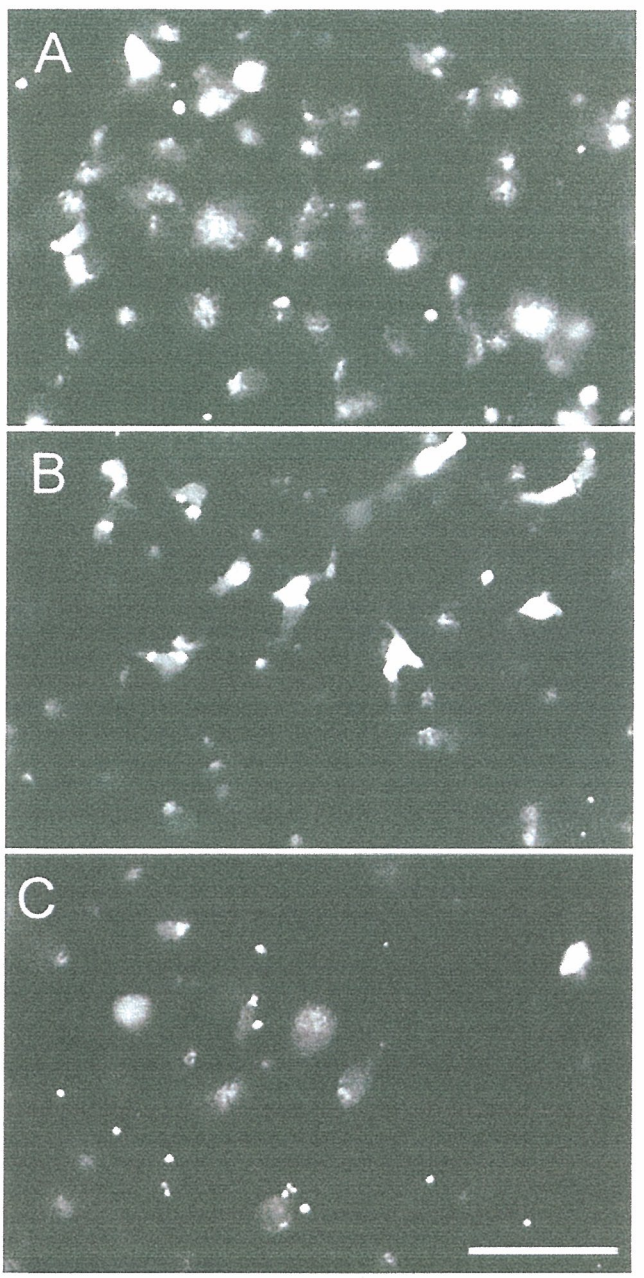

FIGURE 6. Effect of the IGF-1 receptor antagonist JB-3 on neuroprotection by TES. FG-labeled RGCs in the retina 7 days after ON transection. (**A**) Combined treatment with TES and injection of PBS. Combined treatment with TES and daily intraperitoneal injection of (**B**) 10 μg/kg or (**C**) 100 μg/kg JB-3. Scale bar, 25 μm.

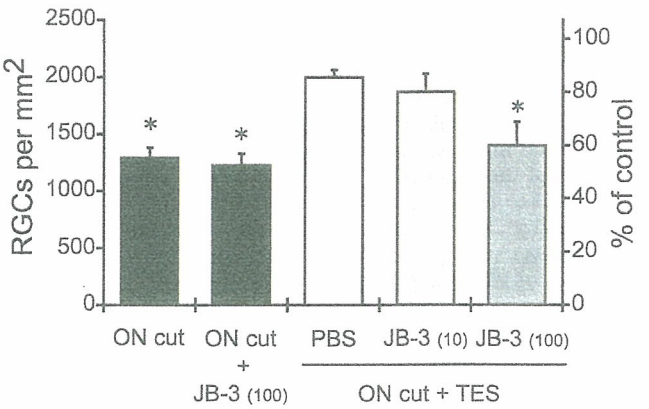

FIGURE 7. Quantitative analysis of the density of surviving RGCs after daily intraperitoneal injections of JB-3 (dose, in micrograms per kilogram per day, shown in parentheses) 7 days after ON transection (n = 4 for each group). Although daily injection of 10 μg/kg JB-3 with TES did not alter the number of surviving RGCs when compared with the treatment combining TES with daily injection of PBS, daily injection of 100 μg/kg JB-3 significantly decreased the number of RGCs. Daily injection of 100 μg/kg without TES, however, did not alter the number of RGCs, compared with ON transection without injection of JB-3 (ON cut). *Statistical significance compared with PBS ($P < 0.05$; one-way ANOVA followed by the Tukey test).

We have demonstrated that electrical stimulation of the stump of the transected ON promoted the survival of axotomized RGCs,[12] and the present study showed that TES, which is less invasive than stimulation of the transected ON, also protects axotomized RGCs from apoptosis. The effect of TES is comparable to that of electrical stimulation to the transected ON.[12] The extent of the neuroprotective effect of TES is also similar to that of intravitreal application of neurotrophic factors.[6,7] The strong effect of TES can be explained by the fact that it upregulated the expression of IGF-1 in the retina for more than 7 days.

Intrinsic Retinal IGF-1 System

IGF-1 has been reported to promote the survival, differentiation, and proliferation of retinal neurons.[38] More specifically, IGF-1 has been reported to promote the survival of injured RGCs, both in vivo[11] and in vitro.[36] In this study, we showed that IGF-1 was recruited from Müller cells by TES and was released to rescue the axotomized RGCs near the Müller cells.

Autocrine-paracrine IGF-1 systems have been reported to exist in the retina.[33,39–42] IGF-1 mRNA was shown to be localized in the GCL in the intact rat retina by in situ hybridization analysis.[33] In contrast, Müller cells express IGF-1 mRNA in vitro.[43] What retinal cells produce and how IGF-1 moves in vivo have not been determined. In the present study, immu-

nohistochemical analyses showed that Müller cells contained small amounts of IGF-1 in their endfeet before TES and that, after TES, Müller cells were activated to increase the level of IGF-1. Our study provides in vivo evidence that the intrinsic IGF-1 paracrine system is in the Müller cells.

The mechanism of the activation of production of IGF-1 by TES has not been determined. It was reported that the regulation of the expression of trophic factors in neurons is clearly linked to their electrical activity. Activation of L-type voltage sensitive Ca^{2+} channels or the non-*N*-methyl-D-aspartate (NMDA) subtype of glutamate receptor leads to an enhancement of BDNF mRNA levels in hippocampal neurons[44,45] and in cortical neurons.[46,47] Similarly, the mechanism for the increased levels of IGF-1 in this study may be related to the electrical activity of retinal neurons and/or glial cells. Further experiments are needed to elucidate this mechanism in detail so that techniques can be designed to stimulate the control glial cells to produce more neurotrophic factors by electrical stimulation.

TES as a New Clinical Technique

Our findings allow us to propose electrical stimulation as a new therapy that activates the intrinsic neuroprotective system. Until now, intravitreal injection or gene transfer of exogenous neurotrophic factors have been used to rescue degenerating retinal neurons[5–11] to provide sustained trophic support. With these methods, however, it is still difficult to deliver exogenous neuroprotective agents chronically into retinal neurons in patients. In addition, intravitreal injection of such neuroprotective agents may cause ocular side effects such as cataract or endophthalmitis. In contrast, TES can control the synthesis of IGF-1, one of the endogenous neurotrophic factors that can then have a neuroprotective effect. This electrical stimulation therapy is simple and less invasive, and ocular side effects were not observed after TES during the course of the study. TES may also have therapeutic or preventive potential in progressive diseases of RGCs, including glaucomatous optic neuropathy. We are now designing a clinical trial using TES for optic neuropathies that are difficult to treat by present methods.

In conclusion, our results showed that TES leads to the upregulation and release of IGF-1 in Müller cells and, consequently, protects the RGCs from secondary cell death after ON transection. Müller cells play an important role in neuroprotection, as well as a housekeeping role that maintains the integrity and the normal function of the retina.

Acknowledgments

The authors thank Yozo Miyake, Hajime Sawai, and Kenji Matsushita for helpful advice and Jun-Sub Choi and Hiroyuki Kanda for technical support.

References

1. Ramon y Cajal S. *Degeneration and Regeneration of the Nervous System.* London: Oxford University Press; 1928.
2. Isenmann S, Kretz A, Cellerino A. Molecular determinants of retinal ganglion cell development, survival, and regeneration. *Prog Retin Eye Res.* 2003;22:483–543.
3. Berkelaar M, Clarke DB, Wang YC, Bray GM, Aguayo AJ. Axotomy results in delayed death and apoptosis of retinal ganglion cells in adult rats. *J Neurosci.* 1994;14:4368–4374.
4. Villegas-Pérez M, Vidal-Sanz M, Raminsky M, Bray G, Aguayo AJ. Rapid and protracted phases of retinal ganglion cell loss follow axotomy in the optic nerve of adult rats. *J Neurobiol.* 1993;24:23–36.
5. Carmignoto G, Maffei L, Candeo P, Canella R, Comelli C. Effect of NGF on the survival of rat retinal ganglion cells following optic nerve section. *J Neurosci.* 1989;9:1263–1272.
6. Mey J, Thanos S. Intravitreal injection of neurotrophic factors support the survival of axotomized retinal ganglion cells in adult rats in vivo. *Brain Res.* 1993;602:304–317.
7. Mansour-Robaey S, Clarke DB, Wang YC, Bray GM, Aguayo AJ. Effects of ocular injury and administration of brain-derived neurotrophic factor on survival and regrowth of axotomized retinal ganglion cells. *Proc Natl Acad Sci USA.* 1994;91:1632–1636.
8. Klöcker N, Braunling F, Isenmann S, Bahr M. In vivo neurotrophic effects of GDNF on axotomized retinal ganglion cells. *Neuroreport.* 1997;8:3439–3442.
9. Clarke DB, Bray GM, Aguayo AJ. Prolonged administration of NT-4/5 fails to rescue most axotomized retinal ganglion cells in adult rats. *Vision Res.* 1998;38:1517–1524.
10. Di polo A, Aigner LJ, Dunn RJ, Bray GM, Aguayo AJ. Prolonged delivery of brain-derived neurotrophic factor by adenovirus-infected Müller cells temporarily rescues injured retinal ganglion cells. *Proc Natl Acad Sci USA.* 1998;95:3978–3983.
11. Kermer P, Klöcker N, Labes M, Bähr M. Insulin-like growth factor-1 protects axotomized rat retinal ganglion cells from secondary death via PI3-K-dependent Akt phosphorylation and inhibition of caspase-3 in vivo. *J Neurosci.* 2000;20:2–8.
12. Morimoto T, Miyoshi T, Fujikado T, Tano Y, Fukuda Y. Electrical stimulation enhances the survival of axotomized retinal ganglion cells *in vivo. Neuroreport.* 2002;13:227–230.
13. Potts AM, Inoue J, Buffum D. The electrically evoked response of the visual system (EER). *Invest Ophthalmol.* 1968;7:269–278.
14. Potts AM, Inoue J. The electrically evoked response of the visual system. 3. Further contribution of the origin of the EER. *Invest Ophthalmol.* 1970;9:814–819.
15. Shimazu K, Miyake Y, Watanabe S. Retinal ganglion cell response properties in the transcorneal electrically evoked response of the visual system. *Vision Res.* 1999;39:2251–2260.
16. Nibuya M, Morinobu S, Duman RS. Regulation of BDNF and trkB mRNA in rat brain by chronic electroconvulsive seizure and antidepressant drug treatments. *J Neurosci.* 1995;15:7539–7547.
17. Al-Majed AA, Brushart TM, Gordon T. Electrical stimulation accelerates and increases expression of BDNF and trkB mRNA in regenerating rat femoral motoneurons. *Eur J Neurosci.* 2000;12:4381–4390.
18. Castren E, Zafra F, Thoenen H, Lindholm D. Light regulates expression of brain-derived neurotrophic factor mRNA in rat visual cortex. *Proc Natl Acad Sci USA.* 1992;89:9444–9448.
19. Bova R, Micheli MR, Qualadrucci P, Zucconi GG. BDNF and trkB mRNAs oscillate in rat brain during the light-dark cycle. *Brain Res Mol Brain Res.* 1998;57:321–324.
20. Nakazawa T, Nakano I, Furuyama T, Morii H, Tamai M, Mori N. The SCG10-related gene family in the developing rat retina: persistent expression of SCLIP and stathmin in mature ganglion cell layer. *Brain Res.* 2000;861:399–407.
21. Yamaguchi A, Taniguchi M, Hori O, et al. Peg3/Pw1 is involved in p53-mediated cell death pathway in brain ischemia/hypoxia. *J Biol Chem.* 2002;277:623–629.
22. Chaum E, Yang H. Transgenic expression of IGF-1 modifies the proliferative potential of human retinal pigment epithelial cells. *Invest Ophthalmol Vis Sci.* 2002;43:3758–3764.
23. Chavez JC, LaManna JC. Activation of hypoxia-inducible factor-1 in the rat cerebral cortex after transient global ischemia: potential role of insulin-like growth factor-1. *J Neurosci.* 2002;22:8922–8931.
24. Smith LE, Shen W, Perruzzi C, et al. Regulation of vascular endothelial growth factor-dependent retinal neovascularization by insulin-like growth factor-1 receptor. *Nat Med.* 1999;5:1390–1395.
25. Pietrzkowski Z, Wernicke D, Porcu P, Jameson BA, Baserga R. Inhibition of cellular proliferation by peptide analogues of insulin-like growth factor-1. *Cancer Res.* 1992;52:6447–6451.
26. Dowling JE. *The Retina: An Approachable Part of the Brain.* Cambridge, MA: Harvard University Press; 1987.

27. Wen R, Song Y, Cheng T, et al. Injury-induced upregulation of bFGF and CNTF mRNAs in the rat retina. *J Neurosci.* 1995;15: 7377–7385.
28. Gao H, Hollyfield JG. Basic fibroblast growth factor: increased gene expression in inherited and light-induced photoreceptor degeneration. *Exp Eye Res.* 1996;62:181–189.
29. Dyer MA, Cepko CL. Control of Müller glial cell proliferation and activation following retinal injury. *Nat Neurosci.* 2000;3:873–880.
30. Chen H, Weber AJ. Expression of glial fibrillary acid protein and glutamine synthetase by Müller cells after optic nerve damage and intravitreal application of brain-derived neurotrophic factor. *Glia.* 2002;38:115–125.
31. Hayry P, Myllarniemi M, Aavik E, et al. Stabile D-peptide analog of insulin-like growth factor-1 inhibits smooth muscle cell proliferation after carotid ballooning injury in the rat. *FASEB J.* 1995;9: 1336–1344.
32. Lin L-F, Doherty D, Lile J, Bektesh S, Collins F. GDNF: a glial cell line-derived neurotrophic factor for midbrain dopaminergic neurons. *Science.* 1993;260:1130–1132.
33. Burren CP, Berka JL, Edmondson SR, Werther GA, Batch JA. Localization of mRNAs for insulin-like growth factor-1 (IGF-1), IGF-1 receptor, and IGF binding proteins in rat eye. *Invest Ophthalmol Vis Sci.* 1996;37:1459–1468.
34. Vecino E, Garcia-Crespo D, Garcia M, Martinez-Millan L, Sharma SC, Carrascal E. Rat retinal ganglion cells co-express brain derived neurotrophic factor (BDNF) and its receptor TrkB. *Vision Res.* 2002;42:151–157.
35. Garcia M, Forster V, Hicks D, Vecino E. In vivo expression of neurotrophins and neurotrophin receptors is conserved in adult porcine retina in vitro. *Invest Ophthalmol Vis Sci.* 2003;44:4532–4541.
36. Meyer-Franke A, Kaplan MR, Pfrieger FW, Barres BA. Characterization of the signaling interactions that promote the survival and growth of developing retinal ganglion cells in culture. *Neuron.* 1995;15:805–819.
37. Shen S, Wiemelt AP, McMorris FA, Barres BA. Retinal ganglion cells lose trophic responsiveness after axotomy. *Neuron.* 1999;23:285–295.
38. Hernández-Sánchez C, López-Carranza A, Alarcón C, de la Rosa EJ, de Pablo F. Autocrine/paracrine role of insulin-related growth factors in neurogenesis: local expression and effects on cell proliferation and differentiation in retina. *Proc Natl Acad Sci USA.* 1995;92:9834–9838.
39. Danias J, Stylianopoulou F. Expression of IGF-I and IGF-II genes in the adult rat eye. *Curr Eye Res.* 1990;9:379–386.
40. Waldbillig RJ, Pfeffer BA, Schoen TJ, et al. Evidence for an insulin-like growth factor autocrine-paracrine system in the retinal photoreceptor-pigment epithelial cell complex. *J Neurochem.* 1991; 57:1522–1533.
41. Moriarty P, Boulton M, Dickson A, McLeod D. Production of IGF-I and IGF binding proteins by retinal cells in vitro. *Br J Ophthalmol.* 1994;78:638–642.
42. Lambooij AC, van Wely KH, Lindenbergh-Kortleve DJ, Kuijpers RW, Kliffen M, Mooy CM. Insulin-like growth factor-1 and its receptor in neovascular age-related macular degeneration. *Invest Ophthalmol Vis Sci.* 2003;44:2192–2198.
43. Li F, Cao W, Steinberg RH, LaVail MM. Basic FGF-induced downregulation of IGF-I mRNA in cultured rat Müller cells. *Exp Eye Res.* 1999;68:19–27.
44. Zafra F, Hengerer B, Leibrock J, Thoenen H, Lindholm D. Activity dependent regulation of BDNF and NGF mRNAs in the rat hippocampus is mediated by non-NMDA glutamate receptors. *EMBO J.* 1990;9:3545–3550.
45. Zafra F, Castren E, Thoenen H, Lindholm D. Interplay between glutamate and gamma-aminobutyric acid transmitter systems in the physiological regulation of brain-derived neurotrophic factor and nerve growth factor synthesis in hippocampal neurons. *Proc Natl Acad Sci USA.* 1991;88:10037–10041.
46. Ghosh A, Carnahan J, Greenberg ME. Requirement for BDNF in activity-dependent survival of cortical neurons. *Science.* 1994;263: 1618–1623.
47. Tao X, Finkbeiner S, Arnold DB, Shaywitz AJ, Greenberg ME. Ca2+ influx regulates BDNF transcription by a CREB family transcription factor-dependent mechanism. *Neuron.* 1998;20:709–726.

Graefe's Arch Clin Exp Ophthalmol
DOI 10.1007/s00417-007-0563-z

CLINICAL INVESTIGATION

Evaluation of phosphenes elicited by extraocular stimulation in normals and by suprachoroidal-transretinal stimulation in patients with retinitis pigmentosa

Takashi Fujikado · Takeshi Morimoto · Hiroyuki Kanda · Shunji Kusaka · Kazuaki Nakauchi · Motoki Ozawa · Kenji Matsushita · Hirokazu Sakaguchi · Yasushi Ikuno · Motohiro Kamei · Yasuo Tano

Received: 4 July 2006 / Revised: 1 February 2007 / Accepted: 17 February 2007

Abstract
Background To determine the efficient parameters to evoke electrical phosphenes is essential for the development of a retinal prosthesis. We studied the efficient parameters in normal subjects and investigated if suprachoroidal-transretinal stimulation (STS) is effective in patients with advanced retinitis pigmentosa (RP) using these efficient parameters.
Methods The amplitude of pupillary reflex (PR) evoked by transcorneal electrical stimulation (TcES) was determined at different frequencies in eight normal subjects. The relationship between localized phosphenes elicited by transscleral electrical stimulation (TsES) and the pulse parameters was also examined in six normal subjects. The phosphenes evoked by STS were examined in two patients with RP with bare light perception. Biphasic pulses (cathodic first, duration: 0.5 or 1.0 ms, frequency: 20 Hz) were applied through selected channel(s). The size and shape of the phosphenes perceived by the patients were recorded.
Results The maximum PR was evoked by TcES with a frequency of 20 Hz. The brightest phosphene was elicited by TsES with a pulse train of more than 10 pulses, duration of 0.5–1.0 ms and a frequency of 20 to 50 Hz. In RP patients, localized phosphenes were elicited with a current of 0.3–0.5 mA (0.5 ms) in patient 1 and 0.4 mA (1.0 ms) in patient 2. Two isolated or dumbbell-shaped phosphenes were perceived when the stimulus was delivered through two adjacent channels.
Conclusion Biphasic pulse trains (≥10 pulses) with a duration of 0.5–1.0 ms and a frequency of 20–50 Hz were efficient for evoking phosphenes by localized extraocular stimulation in normal subjects. With these parameters, STS is a feasible method to use with a retinal prosthesis even in advanced stages of RPs.

Keywords Artificial retina · Retinitis pigmentosa · Phosphene · Pupillary reflex · Suprachoroidal-transretinal stimulation

T. Fujikado · T. Morimoto · H. Kanda · S. Kusaka · K. Nakauchi
Department of Applied Visual Science,
Osaka University Graduate School of Medicine,
Osaka, Japan

H. Kanda · M. Ozawa
Nidek Co.,
Gamagori, Aichi, Japan

K. Matsushita · H. Sakaguchi · Y. Ikuno · M. Kamei · Y. Tano
Department of Ophthalmology,
Osaka University Graduate School of Medicine,
Osaka, Japan

T. Fujikado (✉)
Department of Applied Visual Science,
Osaka University Graduate School of Medicine,
2-2 Yamadaoka, Suita,
Osaka 565-0871, Japan
e-mail: fujikado@ophthal.med.osaka-u.ac.jp

Introduction

Retinitis pigmentosa (RP) is one of the leading causes of blindness in developed countries and is characterized by a progressive degeneration of photoreceptors [15, 20]. In the advanced stage, RP patients have little or no functional vision. To restore some vision of these patients, the strategy

of stimulating the residual retinal neurons by a retinal prosthesis is being extensively studied [14, 31]. Various types of retinal or optic nerve prostheses have been developed, and these have been tested in animals [1, 4, 8, 10, 13, 25, 29, 30] and patients [2, 3, 7, 23]. A typical retinal prosthesis consists of an array of electrodes that is implanted above or beneath the retina and is used to deliver electrical stimulation to the retina to evoke a light sensation called phosphenes.

We have developed a new approach for stimulating the retina called suprachoroidal-transretinal stimulation (STS) [10, 19]. In this method, the retinal prosthesis is placed in a scleral pocket and the reference electrode is inserted into the vitreous. Although the distance between electrodes and the retina is not close compared with other types of artificial retinas, the transretinal currents can stimulate the retina effectively, and the threshold current to evoke electrically evoked potentials by STS is comparable to that by other electrodes [19].

The success of retinal prosthesis to restore vision depends on the presence of physiologically intact retinal ganglion cells (RGCs) that can transmit visual signals to the brain. Morphometric studies of the retinas in RP patients have shown that some of the RGCs are surviving [5, 24, 27]. Postmortem studies of RP eyes have shown that the number of RGC was approximately 30% of that in normal age-matched eyes in the macular area, but only 20% in extramacular regions [5, 24].

Several groups, [16, 21] including our laboratory, have used transcorneal electrical stimulation (TcES) to estimate the residual function of RGCs by the threshold current to evoke phosphenes in RP patients, and our studies have shown that the threshold current to elicit phosphenes was significantly higher in a group of RP patients than in normal subjects [17].

Before investigating the effectiveness of using the STS method to stimulate the retina of RP patients, the efficient parameters to evoke phosphenes by electrical pulses should be determined in normal subjects. This was necessary because it might be difficult to determine the most efficient parameters and retinal loci that would respond to the STS stimulation in RP patients under the acute circumstances of acute experiment. Although the population of retinal neurons that are activated by electrical stimulation could be different between normal subjects and RP patients, the evaluation of efficient parameters in normal subjects should be valuable as a preclinical experiment.

For this, we first studied the effect of the frequency of the TcES stimuli on the pupillary constriction in normal subjects. From this, the efficient frequency to stimulate the retina was determined objectively.

Next, we investigated the effect of localized transscleral electrical stimulation (TsES) on eliciting phosphenes in normal subjects to determine the efficient parameters for localized transretinal stimulation. Finally, using these efficient parameters, we investigated the effectiveness of the STS method to elicit phosphenes in two legally blind patients with RP.

Subjects and methods

Normal subjects and retinitis pigmentosa patients

Eight volunteers (34±6 years; mean age ± SD) with no ocular disorders were enrolled in the TcES study, and six other volunteers (42±9 years) with no ocular disorders were enrolled in the TsES study.

Two patients (both 65 years old) with RP were studied. The diagnosis was confirmed by independent ophthalmological and ERG examinations.

All subjects and patients gave an informed consent after a full explanation of the purpose of this study and the procedures to be used. They were free to withdraw at any time. This study adhered to the Declaration of Helsinki and was approved by the Ethics Committee of Osaka University Hospital.

Transcorneal electrical stimulation

Before the TcES, the cornea was anesthetized with 0.4% oxyburocaine hydrochloride, and the cornea was covered with 3% hyaluronic acid and 4% chondroitin sulfate (Viscoat, Alcon Japan Ltd., Tokyo, Japan) to protect it from mechanical injury by the contact lens electrode. After a dark-adaptation period of 15 min, a concentric, bipolar contact lens electrode (Burian-Allen; Hansen Ophthalmic Laboratories, Iowa City, IA) was placed on the cornea, and electric current pulses (20 pulses) were delivered from a stimulator SEN-7203 (Nihonkoden, Tokyo, Japan) and stimulus isolator unit A395 (WPI, Sarasota, FL) through the two electrodes embedded in the contact lens (Fig. 1a).

The electrical stimuli were rectangular, with a train of 20 biphasic (anodic first) pulses of 10 ms duration without an interpulse delay (Fig. 1a). These parameters that elicited phophenes effectively were chosen based on the results of psychophysical experiments on normal volunteers (Matsushita K et al., ARVO abstract 2003). The current intensity ranged from 25 μA to 250 μA, and the frequency ranged from 5 Hz to 50 Hz.

Recording pupillary constriction

An infrared pupillometer, the IRISCORDER C7364 (HAMAMATSU, Hamamatsu, Japan), was used to record the pupillary responses evoked by light stimuli and by TcES. The subjects wore a goggle equipped with an